

Article

Preparation and Temperature Susceptibility Evaluation of Crumb Rubber Modified Asphalt Applied in Alpine Regions

Youjie Zong, Rui Xiong *, Yaogang Tian, Mingfeng Chang, Xiaowen Wang, Jiahao Yu, Yixing Zhang, Baozhu Feng, Haoyu Wang and Chuang Li

School of Materials Science and Engineering, Chang'an University, Xi'an 710061, China; 2020031003@chd.edu.cn (Y.Z.); ygtian@chd.edu.cn (Y.T.); mfchang99@126.com (M.C.); wangxiaowen20211@163.com (X.W.); jiahao17yu@163.com (J.Y.); 2020131065@chd.edu.cn (Y.Z.); 2019131026@chd.edu.cn (B.F.); 2020231070@chd.edu.cn (H.W.); 2021131065@chd.edu.cn (C.L.)

* Correspondence: xiongr61@126.com

Abstract: In alpine regions, the durability of asphalt pavement is worse due to the harsh climate. However, crumb rubber modified asphalt has the potential to improve the durability of pavement. Based on matrix asphalt, crumb rubber, Trans-Polyoctenamer Rubber Reactive Modifier (TOR), and an orthogonal test, the preparation scheme of crumb rubber modified asphalt suitable for alpine regions was obtained. The crumb rubber was selected 30 mesh, and the content of crumb rubber was 24% of the quality of matrix asphalt. Shearing time was 60 min, and preparation temperature was 205 °C. Shearing rate was 5000 r/min, and optimum TOR content was set as 4.5% of the quality of crumb rubber. The temperature susceptibility of matrix asphalt (JZ), crumb rubber modified asphalt (AR), crumb rubber modified asphalt mixed with TOR (TAR) was investigated. The high temperature performance indexes, including phase angle, the complex modulus index, and rutting factor, and the low temperature performance indexes including creep rate and stiffness modulus, the ratio of creep rate and stiffness modulus, Burgers model parameters, dissipated energy ratio, and the derivative of creep compliance were analyzed in depth with multiple parameters. Meanwhile, the mechanisms of prepared AR and TAR were explored. The results indicate that the PG grading is PG64-22 of JZ, PG70-34 of AR, and PG82-28 of TAR. The deformation resistance of TAR at high temperature is superior to AR. The addition of crumb rubber not only improves the temperature susceptibility, but also enhances its viscoelasticity at low temperatures. After the crumb rubber swell in the asphalt system, the network structures are crosslinked and the physical and chemical effects are produced, such as cracking and repolymerization in the asphalt system. TOR can further enhance the swelling and network crosslinking effects of rubber-asphalt. The TAR has the strongest weather resistance. The study provides guidance for AR and TAR to be used in alpine regions.

Keywords: road engineering; alpine regions; crumb rubber modified asphalt; TOR; temperature susceptibility; microscopic mechanism analysis



Citation: Zong, Y.; Xiong, R.; Tian, Y.; Chang, M.; Wang, X.; Yu, J.; Zhang, Y.; Feng, B.; Wang, H.; Li, C. Preparation and Temperature Susceptibility Evaluation of Crumb Rubber Modified Asphalt Applied in Alpine Regions. *Coatings* **2022**, *12*, 496. <https://doi.org/10.3390/coatings12040496>

Academic Editor: Valeria Vignali

Received: 3 March 2022

Accepted: 4 April 2022

Published: 7 April 2022

Publisher's Note: MDPI stays neutral with regard to jurisdictional claims in published maps and institutional affiliations.



Copyright: © 2022 by the authors. Licensee MDPI, Basel, Switzerland. This article is an open access article distributed under the terms and conditions of the Creative Commons Attribution (CC BY) license (<https://creativecommons.org/licenses/by/4.0/>).

1. Introduction

The alpine region is characterized by low temperature, high altitude, large temperature difference, and intense ultraviolet radiation. The daily temperature difference can reach more than 35 °C. Winds in the mountain pass areas can reach force 10 to 12 [1]. The number of freeze–thaw cycles is as high as 80 times per year. The alternating time of positive and negative temperature is more than 6 months per year [2]. The average relative humidity is only 35 percent, far less than 65 percent in eastern China [3]. Asphalt pavement is rapidly aged under strong ultraviolet radiation. Continuous low temperature action, high and low temperature cycle change, and damage of freeze–thaw and frost heaving make asphalt surfaces crack, and the pavement performances are significantly reduced [2,3]. With the extension of service life, the expressways with excellent pavement performance may

generate various diseases [4,5]. The coupling effects of multiple factors in the environment lead to the aggravation of temperature fatigue of pavement structures and accelerate the fatigue damage and performance degradation of pavement structures and materials. It brings about frequent pavement diseases in early service [6–9]. Meanwhile, the increasing traffic volume proposes a severe test to the stability and durability of the pavement surface in alpine regions [10–12].

With the development and improvement of crumb rubber modified asphalt technology, the application and system are gradually being perfected. Generally, when the crumb rubber content is about 10%, modified asphalt has relatively weak performance improvement. The main purpose of its use is to improve the adhesion of asphalt and aggregate and reduce the temperature sensitivity of asphalt pavement. The crumb rubber modified asphalt is mostly used for asphalt pavements with low traffic volume. When the crumb rubber content is about 15%, the performance of crumb rubber modified asphalt has been significantly improved [13]. The use of crumb rubber modified asphalt can slow down the occurrence of road diseases and improve pavement durability, and the advantages of anti-skid and wear resistance are obtained. It is used for the pavement surface layers of heavy traffic and worse original road condition [13]. The plant-produced crumb rubber asphalt shows good storage stability and satisfying road properties compared to other binders, while the asphalt mixture prepared with plant-produced crumb rubber asphalt shows satisfying road performances. In general, the plant-produced crumb rubber asphalt could be a promising replacement for SBS modified asphalt based on the mixture type evaluated [14,15]. State departments of transportations are currently experimenting with use of ground tire rubber (crumb rubber) in bituminous construction and as a crack sealer [16]. The performances of the recycled asphalt concrete with stable crumb rubber asphalt binder were investigated. Both the normal recycled asphalt mixtures and the stable crumb rubber asphalt recycled asphalt mixtures were prepared with 0%, 30%, or 50% content of the reclaimed asphalt pavement. The stable crumb rubber asphalt is much better than the virgin asphalt in recycling the aged asphalt mixtures, with large reclaimed asphalt pavement content which could reach 50% [17–19]. The microstructure and performance of crumb rubber modified asphalt were explored. The crumb rubber modified asphalt have better performance compared with matrix asphalt. The properties of crumb rubber display significant effects on the performance of crumb rubber modified asphalt. The performance of crumb rubber modified asphalt are improved with the decrease in ash content and the increase in acetone extract. Micrographs of crumb rubber modified asphalt prepared under different conditions showed that, compared with crumb rubber modified asphalt prepared by the traditional preparation process, the scattering state of rubber powder and matrix asphalt in crumb rubber modified asphalt prepared by matrix asphalt preblending process is excellent and even, and a perfect polymer reticular structure is formed in the sample system [20–22].

Crumb rubber modified asphalt mixture can reduce the thickness of pavement surface, the incidences of reflective cracks and temperature shrinkage cracks [14,15]. Meanwhile, crumb rubber comes from waste tire containing high polymers such as natural rubber, which is beneficial for enhancing asphalt performance [23,24]. The use of waste tire is also an environmentally friendly waste material recycling technology, and reduces carbon emissions [25,26]. The mechanical response of two gap-graded asphalt rubber mixtures manufactured by the dry process (AR_{dry}) were evaluated. The observed behavior was compared with that of a similar gap-graded mixture without rubber granulate, used as reference. The results were also compared with analogous asphalt rubber mixes produced elsewhere by the wet process (AR_{wet}). The laboratory results and behavior concluded that mechanical performance of the tested AR_{dry} is better than that measured for the reference blend, and was at the same level of performance as AR_{wet} , provided that a proper mixture design and some construction directives are used [27].

The test sections and physical projects using crumb rubber modified asphalt are involved in south, southwest, and light freezing regions of China. However, research on

the specific preparation process and temperature susceptibility of crumb rubber modified asphalt suitable for alpine regions is scarce. Meanwhile, the final performances of crumb rubber modified asphalt are closely related to the chemical composition of the matrix asphalt, physical and chemical properties of the crumb rubber, such as type, size, amount, etc., and preparation parameters, such as the preparation of temperature, shearing rate, mixing time, etc. [28,29]. Raw materials and preparation process are strictly controlled. The crumb rubber modified asphalt of high quality and best performance is prepared. In addition, the technical application system of crumb rubber modified asphalt in alpine regions is still incomplete. In view of this, preparation and temperature susceptibility evaluations of crumb rubber modified asphalt applied in alpine regions were investigated, and modified mechanisms were analyzed.

2. Materials and Methods

2.1. Materials

Crumb rubber modified asphalt is a complex combination system consisting of SK-90# matrix asphalt, crumb rubber, and admixtures. The performance of each raw material has important influences on the performance indexes of crumb rubber modified asphalt. This section mainly studies the properties of SK-90# matrix asphalt, crumb rubber, and admixtures.

2.1.1. Matrix Asphalt

The SK-90# matrix asphalt was used in alpine regions. Table 1 shows its technical indicators, and Figure 1 shows the diagrams of atomic force microscope, which was made by Park Systems in Suwon, Korea. The dispersion phases with peak structure are evenly distributed on the asphalt surface. The structures are thought to be the rise and fall of asphalt in a flat area, which are represented by “spikes” in the three-dimensional diagram. The “bee-structure” of SK-90# matrix asphalt mainly comes from asphaltene and some colloid in the asphalt. The wax elements in asphalt will crystallize at the tip of the “bee-structure”, which is not conducive to the adhesion of asphalt and aggregates. The R_q of root mean square roughness is 6.73 nm calculated.

Table 1. Technical indicators of SK-90# matrix asphalt.

Test Items	Unit	Results	Technical Requirements	Methods
Penetration (25 °C, 100 g, 5 s)	0.1 mm	94.5	80~100	T0604
Ductility (15 °C, 5 cm/min)	cm	>150	≧100	T0605
Softening Point (R&B)	°C	46.0	≧44	T0606
Solubility	%	99.6	≧99.5	T0607
Brookfield viscosity (135 °C)	Pa·s	1.885	-	T0625
Flash point	°C	260	≧245	T0611
Specific gravity	g/cm ³	1.030	Measured value	T0603
RTFOT	Mass loss	%	±0.8	T0610
(163 °C, 75 min)	Ductility (10 °C)	cm	≧8	T0605
	Penetration ratio (25 °C)	%	≧57	T0604

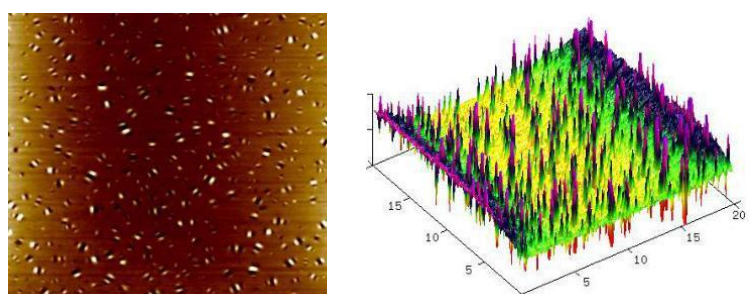


Figure 1. The atomic force microscope images of SK-90# matrix asphalt.

2.1.2. Crumb Rubber

Waste truck radial tire was used as raw material to prepare crumb rubber by normal temperature grinding process. Figure 2 shows the structure of load radial tire, and Table 2 shows the differences in material compositions of different tires by test analysis.

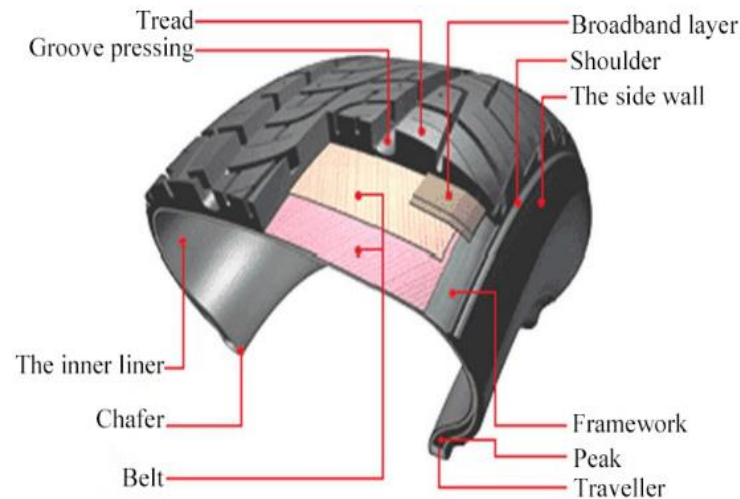


Figure 2. The structure of load radial tire.

Table 2. Comparison of tire composition between car and truck.

Tire Type	Material Content (%)						
	Rubber	Black Carbon	Metal	Fabric	Zinc Oxide	Sulphur	Additive
Car	48	22	15	5	5	1	4
Truck	43	21	27	-	2	1	6

Figure 3 shows the grinding process at normal temperature. As the crumb rubber particles have an irregular shape and large relative specific surface area by the grinding process. It is conducive to full interaction with asphalt, and the cost is the lowest [30,31].

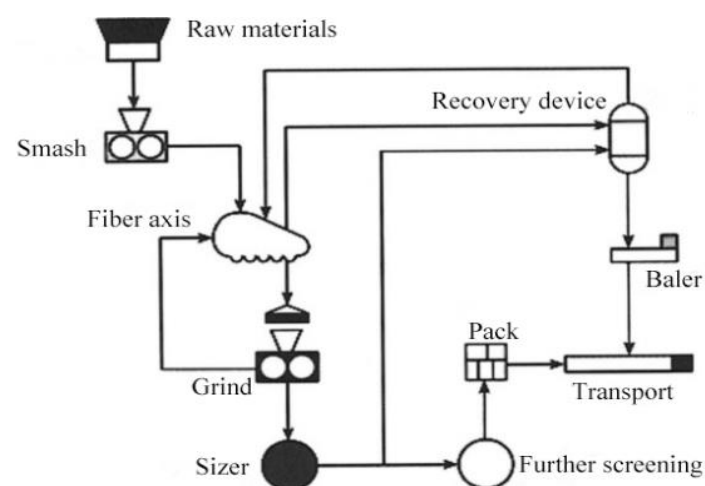


Figure 3. The grinding process at normal temperature.

The crumb rubber images of a scanning electron microscope (SEM) and an infrared spectrum are shown in Figures 4 and 5. Hitachi S-4800 cold field emission scanning electron microscope was made by Japanese high-tech manufacturer, and Fourier transform infrared spectrometer (BRUKER TENSOR II) was made by Germany. Wave numbers of 2958 and 2917 cm^{-1} are the results of stretching vibration of C-H bond in $-\text{CH}_3$ and $-\text{CH}_2-$. In total,

2848 cm^{-1} is produced by symmetric expansion of $-\text{CH}_2-$; 1655 cm^{-1} is produced by the vibration of $\text{C}=\text{O}$ double bond in the carboxy group; 1448 cm^{-1} is produced by the variable angle vibration of $-\text{CH}_2-$; and 1092 cm^{-1} is produced by the scaling of $\text{C}-\text{O}$. The wave number 1539 cm^{-1} is the stretching vibration result of NO_2 in the $\text{R}-\text{NO}_2$. The wave numbers of 743, 834, and 1375 cm^{-1} are generated by out-of-plane and in-plane bending vibration of the benzene torus. The wave number of 965 cm^{-1} is produced by the out-of-plane bending vibration of the $\text{C}-\text{H}$ bond in the trans unsaturated group of butadiene. The main components of crumb rubber are natural rubber and styrene-butadiene rubber. The technical specifications are shown in Tables 3 and 4.

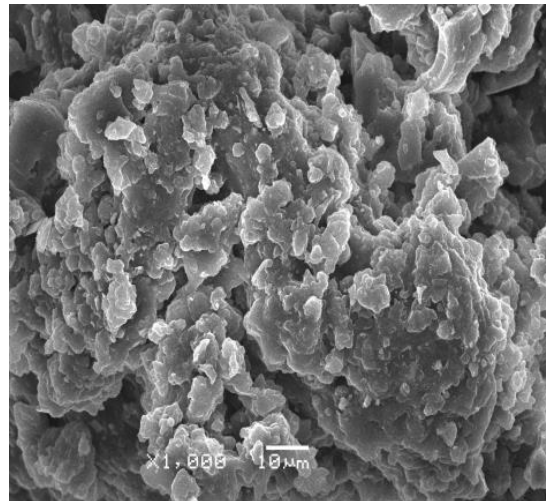


Figure 4. The SEM image of crumb rubber ($\times 1000$).

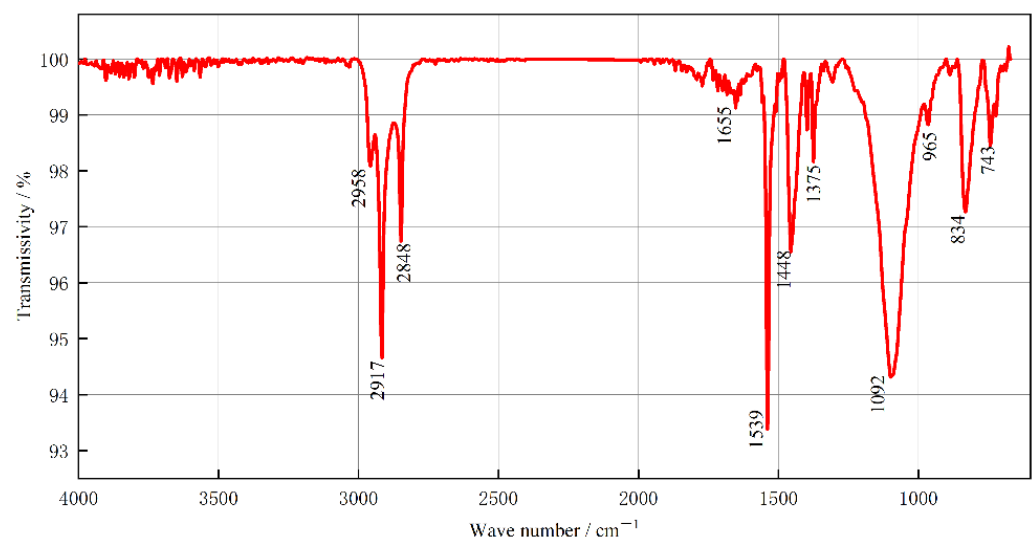


Figure 5. The infrared spectrum diagram of crumb rubber.

Table 3. Physical indicators of crumb rubber.

Index	Metal Content (%)	Fiber Content (%)	Moisture Content (%)	Relative Density
Technical requirements ^①	≤ 0.05	≤ 1	≤ 1	1.10~1.30
Test results	0.023	0	0.3	1.20

^① Reference standard <Ground vulcanized rubber of scrap tires for highway engineering> (JT/T 797-2011).

Table 4. Chemical indicators of crumb rubber.

Index	Rubber Hydrocarbon Content (%)	Ash Content (%)	Acetone Extract (%)	Carbon Black Content (%)
Technical requirements ^①	≥42	≤8	≤22	≥28
Test results	57.5	6.9	12.1	31.5

^① Reference standard <Ground vulcanized rubber of scrap tires for highway engineering> (JT/T 797-2011).

2.1.3. Trans-Polyoctenamer Rubber Reactive Modifier

Trans-Polyoctenamer Rubber Reactive Modifier (TOR) is a polymer with a double bond structure. As shown in Figure 6, TOR is translucent crystalline particles. TOR crosslinks the sulfur in the asphalt to the sulfur on the crumb rubber surface. The network structures of rings and chains of polymers are formed.

**Figure 6.** The macro morphology of TOR.

Figure 7 shows the infrared spectrum diagram of TOR. TOR is mainly composed of saturated and unsaturated carbon chains. The absorption peak of TOR is produced by the antisymmetric absorption vibration of C–H bond in methylene CH₂– at 2917 cm^{−1}. In total, 2849 cm^{−1} is the symmetric vibration effect of C–H in alkane and cycloalkane. The absorption peak of 1467 cm^{−1} is the bending vibration in C–H bond plane. The wave number of 965 cm^{−1} is produced by the out-of-plane bending vibration of the C–H bond in the trans unsaturated group of butadiene. The in-plane wobble vibration produced by saturated methylene is approximately 719 cm^{−1}. The technical specifications are shown in Table 5.

Table 5. Technical indicators of TOR.

Test Item	Unit	Result	Method
Molecular weight (GPC)	/	90,000	Acc-DIN55672-1
Glass-transition temperature (Tg)	°C	−65	ISO 11357
Crystallinity (23 °C)	%	−30	ISO 11357
Melting point	°C	54	ISO 11357
Thermal decomposition (TGA)	°C	275	ISO 11357
Cis/trans double bond ratio	%	20/80	SOP 0188
Mooney viscosity	/	<10	ASTM D1646
Ash content	%	≤0.1	DIN535568.Part1
Volatile substance (1 h, 105 °C)	%	≤0.5	ISO 248
Density (23 °C)	g/cm ³	0.910	ISO 1183

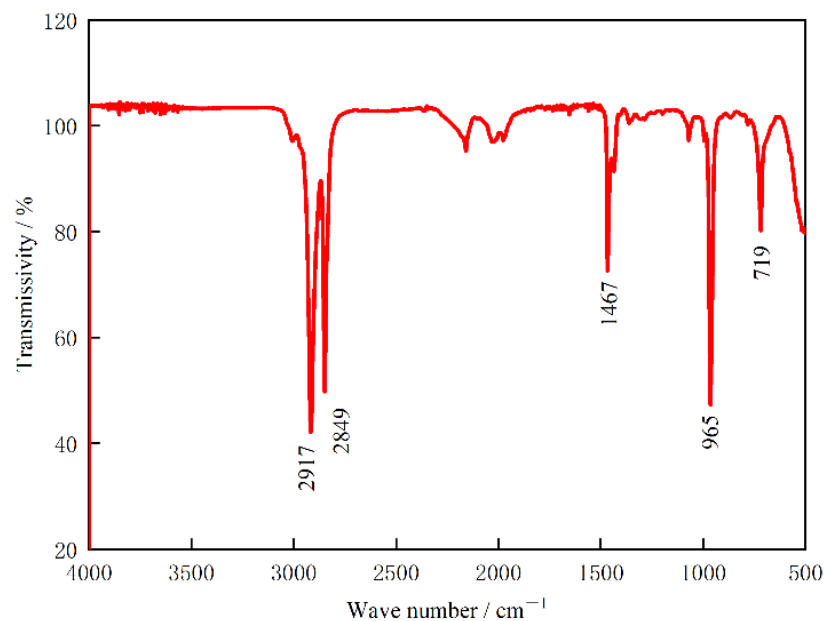


Figure 7. The infrared spectrum diagram of TOR.

2.2. Methods

2.2.1. Preparation Method of Crumb Rubber Modified Asphalt

The matrix asphalt selected SK-90#. It was referred to as JZ. Crumb rubber modified asphalt was referred as AR. When TOR was added, crumb rubber modified asphalt was referred as TAR.

In order to prepare crumb rubber modified asphalt suitable for pavement in alpine regions, the orthogonal test method was adopted. Penetration (25 °C, 100 g, 5 s), softening point, ductility (5 °C), segregation softening point difference (48 h, 163 °C), elastic recovery rate (25 °C), the $|B|$ value of viscosity–temperature regression coefficient, and shearing strength (25 °C) were selected as evaluation indexes. According to Equation (1), the shearing strength was obtained through cone penetration test. The cone penetration value of crumb rubber modified asphalt was tested by cone penetration tester, as shown in Figure 8. $|B|$ values were acquired by Equation (2) and regression analysis of crumb rubber modified asphalt viscosity with temperatures of 135, 150, 165, 180, and 195 °C.

$$\tau = \frac{981Q\cos^2\left(\frac{\alpha}{2}\right)}{\pi h^2 \tan\left(\frac{\alpha}{2}\right)} \quad (1)$$

in which τ is shearing strength, kPa; Q is total mass of conical needle, connecting rod and weights, 195 g; h is cone penetration, mm; and α is the angle of cone tip, 30°.

$$\eta = Ae^{B/T} \quad (2)$$

in which η is viscosity, Pa·s; T is the absolute temperature, K; and A and B are constants. $|B|$ is viscosity–temperature regression coefficient.

The crumb rubber mesh, crumb rubber content, shear time, preparation temperature, and shear rate were taken as the main influencing factors. A four-level table of five factors (A , B , C , D , and E) was listed, as shown in Table 6. The orthogonal table L16 (45) and test scheme are listed in Table 7.

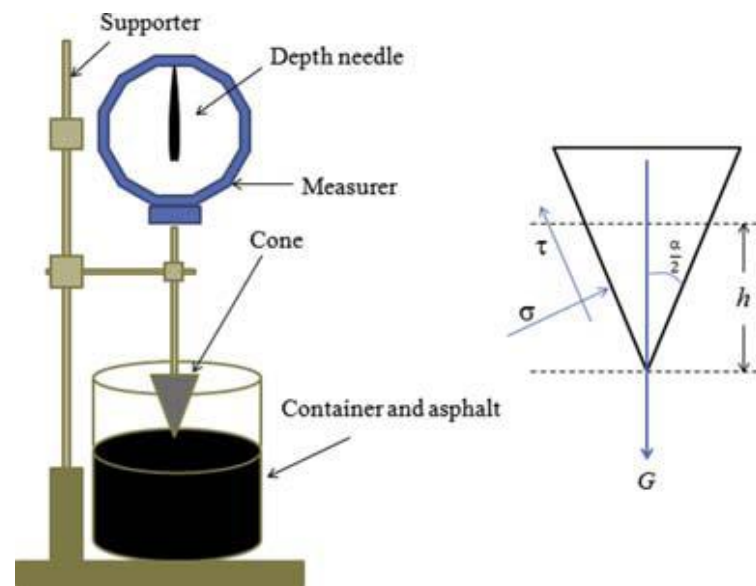


Figure 8. Cone penetration tester.

Table 6. Factor and level of orthogonal test.

Level	Factor				
	A/Crumb Rubber (Mesh)	B/Crumb Rubber Content (%)	C/Shear Time (min)	D/Preparation Temperature (°C)	E/Shear Rate (τ/min)
1	25	12	45	175	3500
2	40	16	60	190	4000
3	60	20	75	205	4500
4	80	24	90	220	5000

Table 7. Orthogonal test scheme.

Scheme	Crumb Rubber (Mesh)	Content (%)	Shear Time (min)	Preparation Temperature (°C)	Shear Rate (τ/min)
1	25	12	45	175	3500
2	25	16	60	190	4000
3	25	20	75	205	4500
4	25	24	90	220	5000
5	30	12	60	205	5000
6	30	16	45	220	4500
7	30	20	90	175	4000
8	30	24	75	190	3500
9	40	12	75	220	4000
10	40	16	90	205	3500
11	40	20	45	190	5000
12	40	24	60	175	4500
13	60	12	90	190	4500
14	60	16	75	175	5000
15	60	20	60	220	3500
16	60	24	45	205	4000

According to the orthogonal test scheme, the preparation process of crumb rubber modified asphalt is shown in Figure 9. On the basis of Standard Test Methods of Bitumen and Bituminous Mixtures for Highway Engineering (JTG E20—2011) and test results, the best preparation process and parameters were determined.

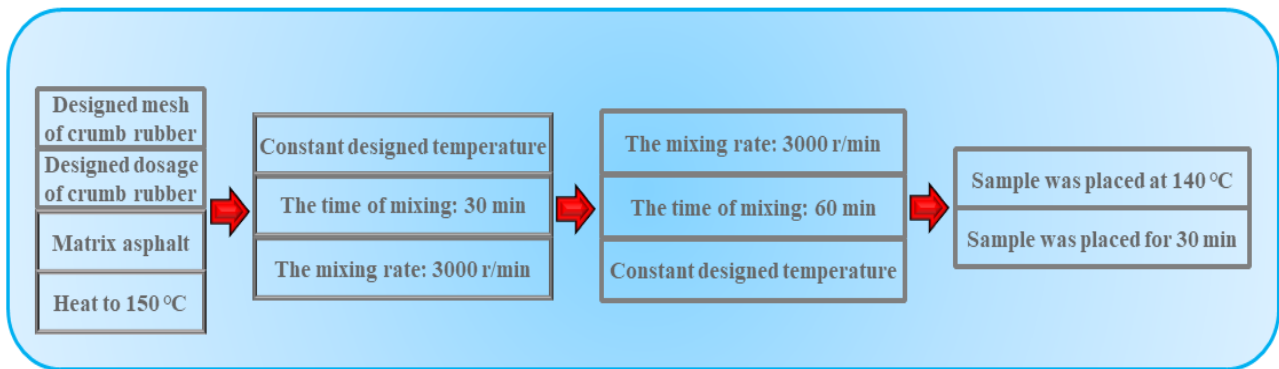


Figure 9. The preparation process of crumb rubber modified asphalt.

2.2.2. Determination of TOR Content

TOR was added to improve pavement performance of crumb rubber modified asphalt. TOR was 0, 4.0%, 4.5%, or 5.0% of the content of crumb rubber. This is represented as W_0 , $W_{4.0}$, $W_{4.5}$, or $W_{5.0}$, respectively. According to Standard Test Methods of Bitumen and Bituminous Mixtures for Highway Engineering (JTG E20-2011), the experiments of penetration, softening point, ductility, elastic recovery rate, cone penetration, segregation softening point difference, and Brinell viscosity at 135, 150, 165, 180, and 195 °C were conducted. The optimal content of TOR was determined in crumb rubber modified asphalt. Meanwhile, shear strength is converted from the cone penetration, according to Equation (1). The Viscosity–Temperature–Susceptibility was calculated by Equation (2).

2.2.3. Dynamic Shear Rheological Test

Referring to AASHTO-TP5 test method, the dynamic shear rheological test was carried out by DHR-1 dynamic shear rheometer. The strain control mode was selected. The strain value was 8%. The frequency was 10 rad/s. The temperature scanning test was carried out in the temperature range of 46–82 °C. Through comparative analysis of phase angle, the complex modulus index GTS, and rutting factor, the effects of crumb rubber and TOR on the high temperature performance of crumb rubber modified asphalt were investigated.

2.2.4. Bending Beam Rheometer Test

The bending beam rheometer is used to test the low temperature performance of asphalt samples. After the three kinds of asphalt samples were aged by TFOT and PAV, the beam samples were prepared. Its length, width, and thickness were 127 ± 2.0 , 12.7 ± 0.1 , and 6.4 ± 0.1 mm, respectively. The test temperature of JZ was set to 6, −12, and −18 °C. The test temperature of AR/TAR were set to −12, −18, −24, and −30 °C. The stiffness modulus and creep rates of different asphalt were obtained by testing under constant stress of 240 s and set temperature. The stiffness modulus and creep rate were calculated by Equations (3) and (4), respectively [32–34].

$$S(t) = \frac{Pl^3}{4bh^3v(t)} \quad (3)$$

$$m = d \times \log(S(t))/d \times \log(t) \quad (4)$$

in which S is stiffness modulus, MPa; m is creep rate; l is the span of the beam, mm; $v(t)$ is deformation of beam midpoint at some moment, mm; h is the height of the beam, mm; p is the constant load, N; and b is the width of the beam, mm.

2.2.5. Microcosmic Test of Crumb Rubber Modified Asphalt

The prepared JZ, AR, and TAR were placed under a fluorescence microscope, scanning electron microscope, and Fourier infrared spectrometer, respectively. The magnifications of

the scanning electron microscope and Fourier microscope were selected 1000 and 5000 times, respectively. The magnification of fluorescence microscope is 100 times. The microstructures of three kinds of asphalts were observed, and mechanisms were analyzed. Figure 10 shows flow chart of material preparations and experimental programs.

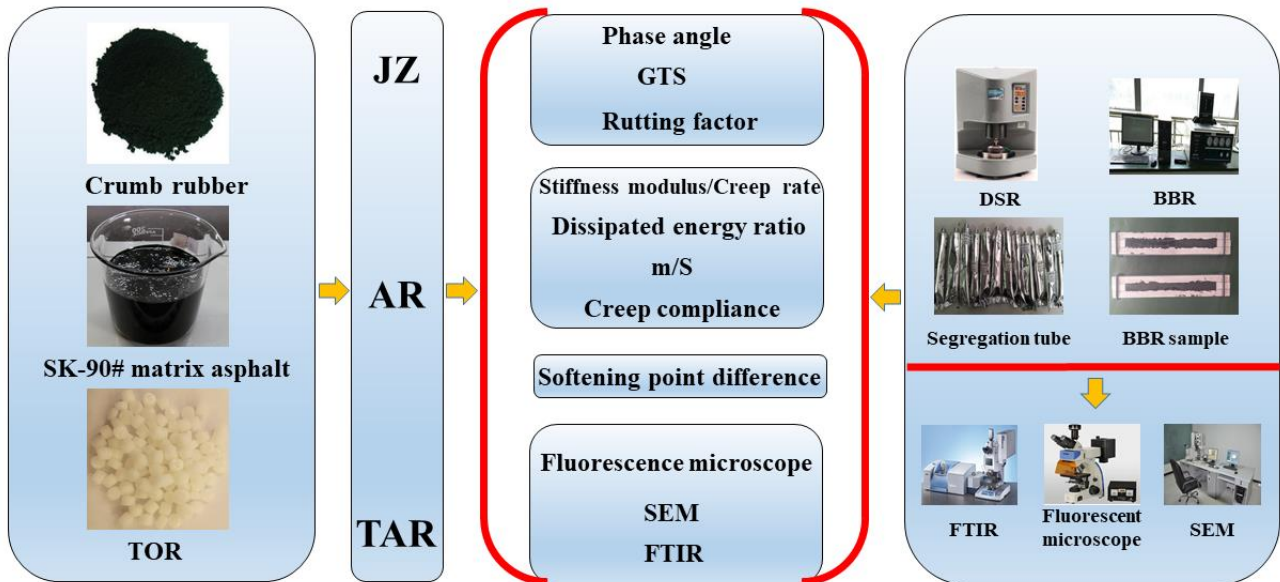


Figure 10. Flow chart of material preparations and experimental programs.

3. Results and Discussion

3.1. Preparation of Crumb Rubber Modified Asphalt

3.1.1. Analysis of Orthogonal Test Results

According to the designed orthogonal test scheme, 16 groups of crumb rubber modified asphalt were prepared. Test results are shown in Table 8.

Table 8. Orthogonal test results.

Number	Penetration (25 °C, 100 g, 5 s) (0.1 mm)	Ductility (15 °C, 5 cm/min) (cm)	Softening Point (°C)	Elastic Recovery Rate (%)	Cone Penetration of 25 °C (cm)	Segregation Softening Point Difference (°C)	Viscosity of 180 °C (cp)	B Value	Shearing Strength (kPa)
1	53.2	8.9	57.4	56	48.3	3.6	537.5	788.4	70.3
2	54.2	11.5	59.8	71	53.2	5.3	1040.0	772.2	58.4
3	77.3	13.2	54.2	43	71.6	3.2	830.0	862.2	32.8
4	85.4	16.9	53.7	38	82.6	3.0	675.0	725.6	24.4
5	67.7	9.6	54.2	56	58.5	0.6	395.0	673.4	48.2
6	73.4	11.2	54.4	71	64.2	8.7	520.0	766.7	40.9
7	52.7	12.0	62.8	68	48.9	6.7	1815.0	896.3	68.4
8	58.9	13.8	63.6	78	50.3	3.7	1775.0	814.0	64.1
9	78.1	12.2	52.6	66	67.4	4.8	342.5	761.0	36.0
10	81	14.2	52.3	54	73.2	3.1	307.5	814.9	30.5
11	84.1	16.6	52.7	58	76.9	5.3	530.0	821.6	28.4
12	46.5	12.5	66.4	82	37.1	2.6	2160.0	749.1	118.3
13	74.4	10.6	50.3	42	64.5	1.3	172.5	872.1	40.7
14	85.3	12.0	50.9	78	12.2	3.1	307.5	761.1	27.3
15	84.2	14.2	51.2	64	76.1	5.4	390.0	798.1	28.2
16	87.4	17.7	54.0	70	72.9	4.4	852.5	800.1	31.1

The range values of penetration, softening point, ductility, segregation softening point difference, elastic recovery rate, $|B|$ value, and shearing strength were analyzed. The range values of various factors and the effects of factor level on the corresponding index were calculated, with the results shown in Table 9.

Table 9. Range values of corresponding indexes under various experimental factors.

Factor	Penetration (25 °C, 100 g, 5 s) (0.1 mm)	Ductility (15 °C, 5 cm/min) (cm)	Softening Point (°C)	Elastic Recovery Rate (%)	Viscosity (cp)	Segregation Softening Point Difference (°C)	$ B $ Value	Shearing Strength (KPa)
A/Powder mesh	19.7	2.2	7.2	16.3	695.6	1.4	21.2	23.5
B/Powder content	6.4	5.0	5.1	13.5	1003.8	2.6	72.3	20.5
C/shear time	11.6	1.7	3.3	17.8	386.3	2.0	79.0	23.3
D/Preparation temperature	20.7	1.8	6.4	15.2	653.9	2.7	57.1	38.8
E/Shear rate	12.8	1.9	3.5	11.3	535.6	2.3	67.2	25.5

The performances of crumb rubber modified asphalt prepared under different combination schemes are different. The crumb rubber mesh has the most significant effect on the softening point value. The softening point values of crumb rubber modified asphalt prepared by 30 mesh and 40 mesh crumb rubber are higher. However, the softening point value of crumb rubber modified asphalt prepared by 60 mesh crumb rubber is minimal. The content of crumb rubber has a significant effect on the low temperature ductility and viscosity of crumb rubber modified asphalt. When the content of crumb rubber is 24%, the ductility and viscosity are about 1.5 times and 3 times higher, respectively, than those of the 12% sample. Therefore, the high content of crumb rubber is beneficial to improve the low temperature performance. Shear time has the most effect on elastic recovery rate and $|B|$ value. With the extension of shear time, elastic recovery rate first increases and then decreases, while the $|B|$ value is the opposite. When shear time is 60 min, elastic recovery rate is the strongest and temperature sensitivity is the lowest. Preparation temperature significantly affects the penetration, segregation softening point difference, and shear strength of the crumb rubber modified asphalt. With the increase in preparation temperature, the penetration gradually increases, and it is also affected by the crumb rubber mesh. The segregation softening point difference first decreases and then increases with the increase in the preparation temperature, and the minimum value is obtained when the preparation temperature is 205 °C. The shear strength decreases significantly with the increase in the preparation temperature. The reason is that the effect of temperature will lead to desulfurization of crumb rubber in asphalt. The shear rate has no significant effect on the performances of crumb rubber modified asphalt.

According to performance requirements of crumb rubber modified asphalt in alpine regions, proper analysis were conducted for penetration, softening point, ductility and elastic recovery rate, segregation softening point difference, shearing strength, and $|B|$ value. The optimal combination schemes required by composite corresponding indexes were selected, as shown in Table 10.

The optimal combination schemes for the preparation of crumb rubber modified asphalt is A₂-B₄-C₂-D₃-E₄, that is, the crumb rubber mesh is 30. The content of crumb rubber is 24%. The shear time is 60 min. The preparation temperature is 205 °C, and the shear rate is 5000 r/min. The confirmed process flow charts of preparation of crumb rubber modified asphalt are shown in Figure 11.

Table 10. Analysis and summary of orthogonal test results.

Index	Factors Influence the Order of Significance	Optimal Portfolio
Penetration	D/Preparation temperature > A/Powder mesh > E/Shear rate > C/shear time > B/Powder content	A ₄ -B ₃ -C ₃ -D ₄ -E ₄
Ductility	B/Powder content > A/Powder mesh > E/Shear rate > D/Preparation temperature > C/shear time	A ₃ -B ₄ -C ₁ -D ₃ -E ₄
Softening point	A/Powder mesh > D/Preparation temperature > B/Powder content > E/Shear rate > C/shear time	A ₂ -B ₄ -C ₂ -D ₁ -E ₂
Elastic recovery rate	C/shear time > A/Powder mesh > D/Preparation temperature > B/Powder content > E/Shear rate	A ₂ -B ₄ -C ₂ -D ₂ -E ₂
Viscosity	B/Powder content > A/Powder mesh > D/Preparation temperature > E/Shear rate > C/shear time	A ₄ -B ₁ -C ₁ -D ₄ -E ₄
Segregation softening point difference	D/Preparation temperature > B/Powder content > E/Shear rate > C/shear time > A/Powder mesh	A ₄ -B ₁ -C ₂ -D ₃ -E ₄
B value	C/shear time > B/Powder content > D/Preparation temperature > E/Shear rate > A/Powder mesh	A ₁ -B ₄ -C ₂ -D ₃ -E ₄
Shearing strength	D/Preparation temperature > E/Shear rate > A/Powder mesh > C/shear time > B/Powder content	A ₂ -B ₄ -C ₂ -D ₁ -E ₃

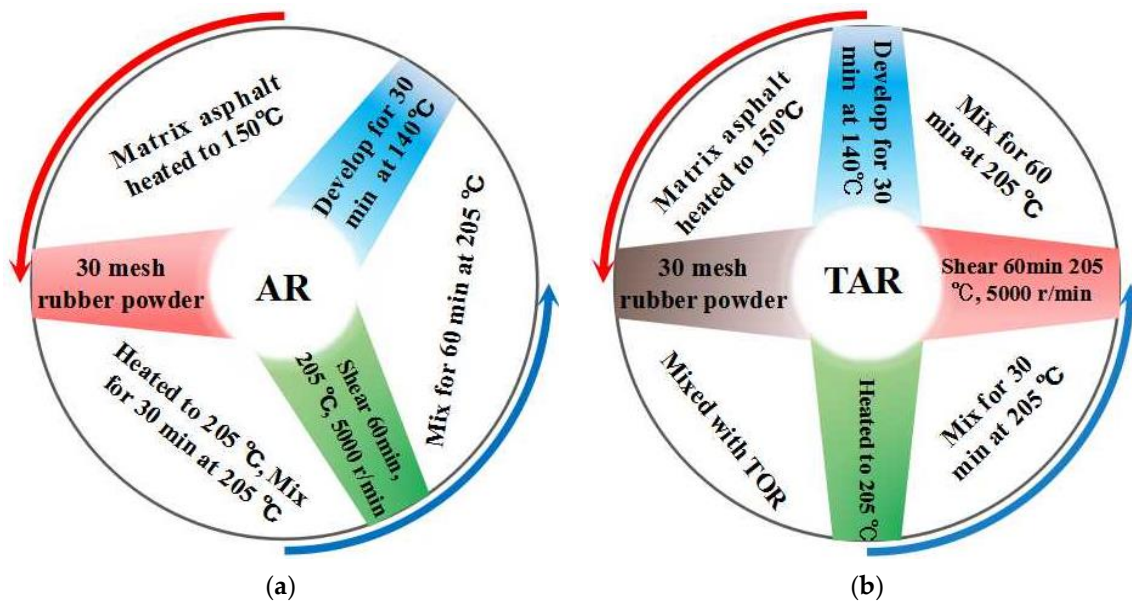


Figure 11. Flow charts of AR and TAR preparation process. (a) AR, (b) TAR.

3.1.2. Determination of TOR Content

When the content of TOR is different, the performances of crumb rubber modified asphalt is shown in Figures 12 and 13. In Figure 12, the softening point, elastic recovery rate, and shear strength of crumb rubber modified asphalt enhance with the increase in TOR, while the penetration, low temperature ductility, segregation softening point difference, and VTS decrease, indicating that TOR significantly improved the flexibility, temperature susceptibility, and storage stability of crumb rubber modified asphalt at low temperatures. With the increase in TOR content, the elastic recovery rate increases by 1%, 7%, and 10%, respectively. The shear strength increases by 5%, 51%, and 79%, respectively. The VTS decreases by 1%, 6%, and 9%, respectively. The difference of segregation softening point decreases by 9%, 8%, and 7%, respectively. When the content of TOR is 4.5%, all the evaluation indexes change significantly. When the content of TOR increases from 4.5% to 5%, the difference of the segregation softening point increases from 0.7 to 1.2, and the

viscosity at 150 °C increases from 4700 to 6075 cp, as shown in Figure 13. Considering the high viscosity, poor storage stability of crumb rubber modified asphalt, the climate of alpine regions, and economical analysis, the appropriate TOR content is determined to be 4.5%.

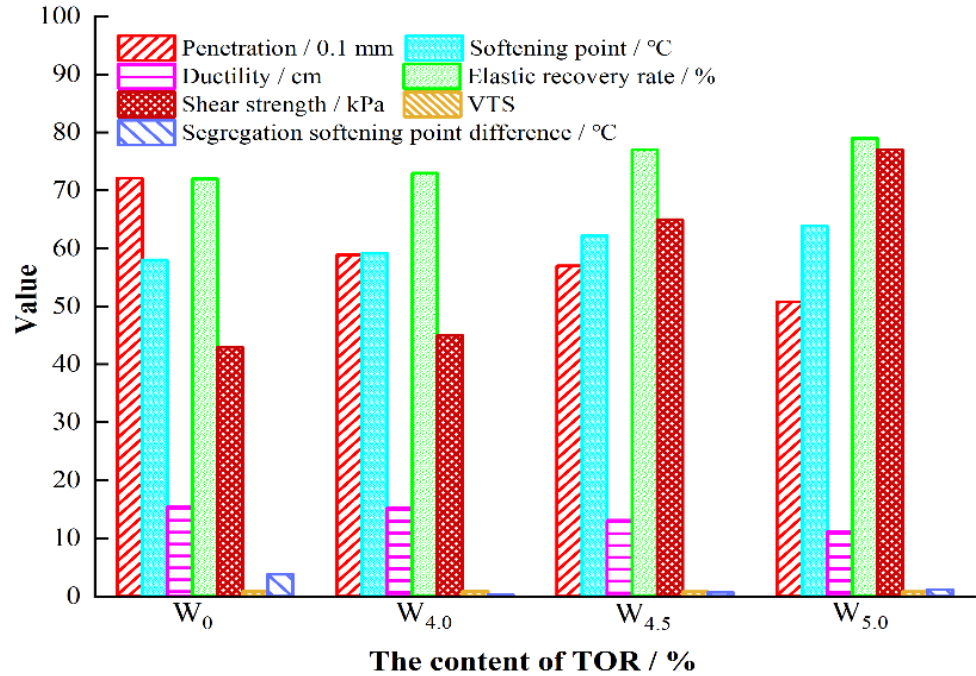


Figure 12. Performance indexes of crumb rubber modified asphalt with different TOR content.

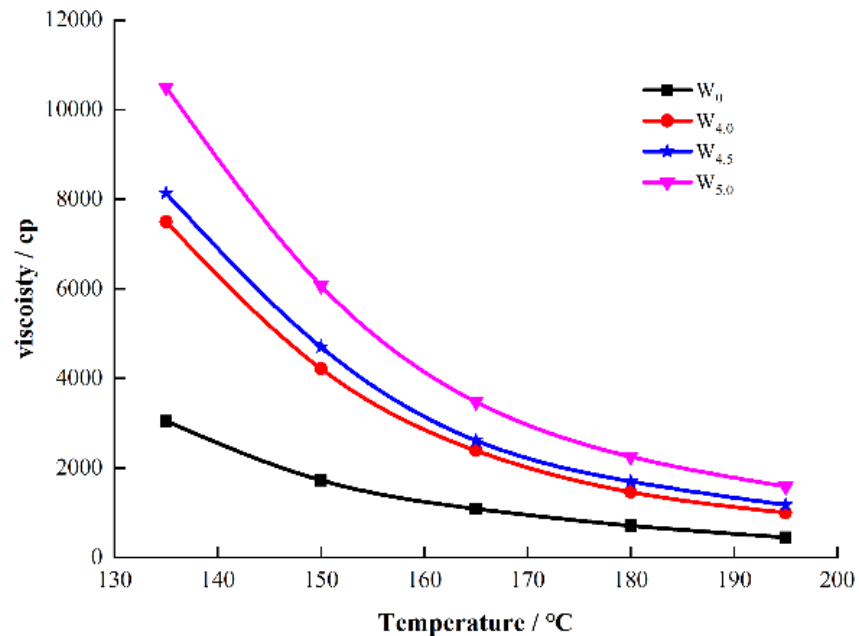


Figure 13. Viscosity of crumb rubber modified asphalt with different TOR content.

3.2. Investigation on High Temperature Performance of Asphalt

3.2.1. Phase Angle

The parameters of dynamic shear rheological test were performed in the temperature range of 46–82 °C. The strain value was 8%, and the frequency was 10 rad/s. The results are shown in Figure 14.

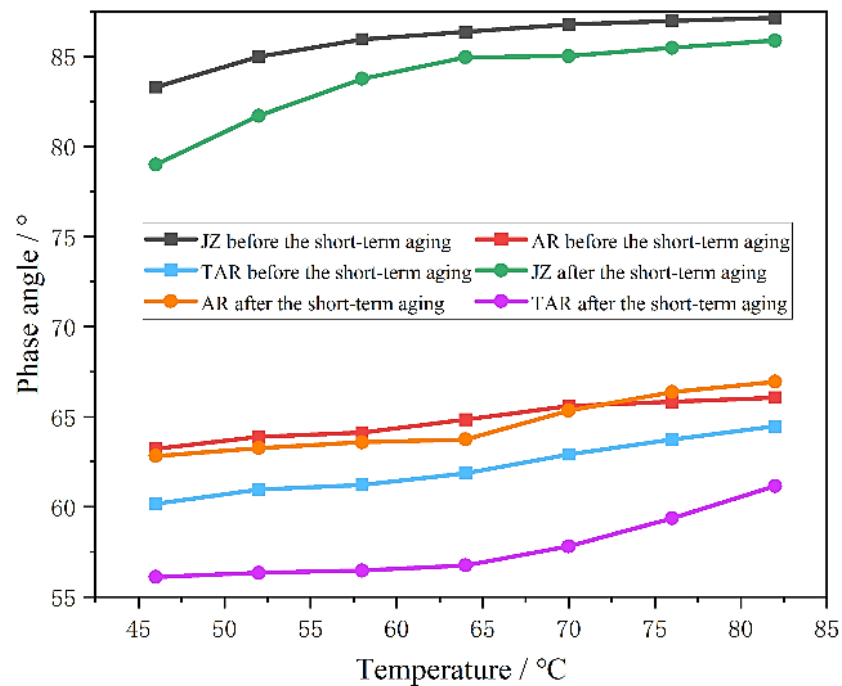


Figure 14. Phase angle.

As shown in Figure 14, the values of phase angle gradually increase as the temperature increases. Under the same temperature, the values of phase angle are $JZ > AR > TAR$. The delay time of asphalt response to stress is affected by asphalt type and temperature condition. When the temperature is 64 °C, the δ_{AR}/δ_{JZ} and δ_{TAR}/δ_{JZ} are 0.76 and 0.72, respectively, before the short-term aging. The reason is that the incorporation of crumb rubber increases the elastic components in the complex modulus of asphalt. The high temperature deformation resistance of asphalt under load is enhanced. The addition of TOR further enhances the effect. After short-term aging, the phase angles of the three kinds of asphalts decrease; δ_{AR}/δ_{JZ} and δ_{TAR}/δ_{JZ} are 0.75 and 0.67, respectively. Meanwhile, the light components of asphalt volatilize. The asphalts become hardened by oxidation. The elastic components of asphalt increase, and the phase angles decrease. The significant order of short-term aging effect on the three kinds of asphalts is $TAR > AR = JZ$.

3.2.2. Complex Modulus Exponent

The complex modulus exponent method is used to characterize the temperature sensitivity of medium and high temperature regions of asphalt by dynamic shear rheometer test. The complex modulus exponent was calculated by Equation (5) [35–37].

$$\lg(\lg G^*) = GTS \times \lg T + C \tag{5}$$

in which G^* is complex modulus, Pa; GTS is the complex modulus exponent; C is constant; and T is the test temperature, K.

Dynamic shear rheometer was used to test the rheological properties of asphalt samples at 58, 64, 70, 76, and 82 °C. Figure 15 shows the regression equations of GTS and regression coefficient results. The greater the absolute value of GTS , the greater the temperature sensitivity of asphalt. The complex modulus G^* double logarithms of the three kinds of asphalts have good linear relationships with the temperature logarithm.

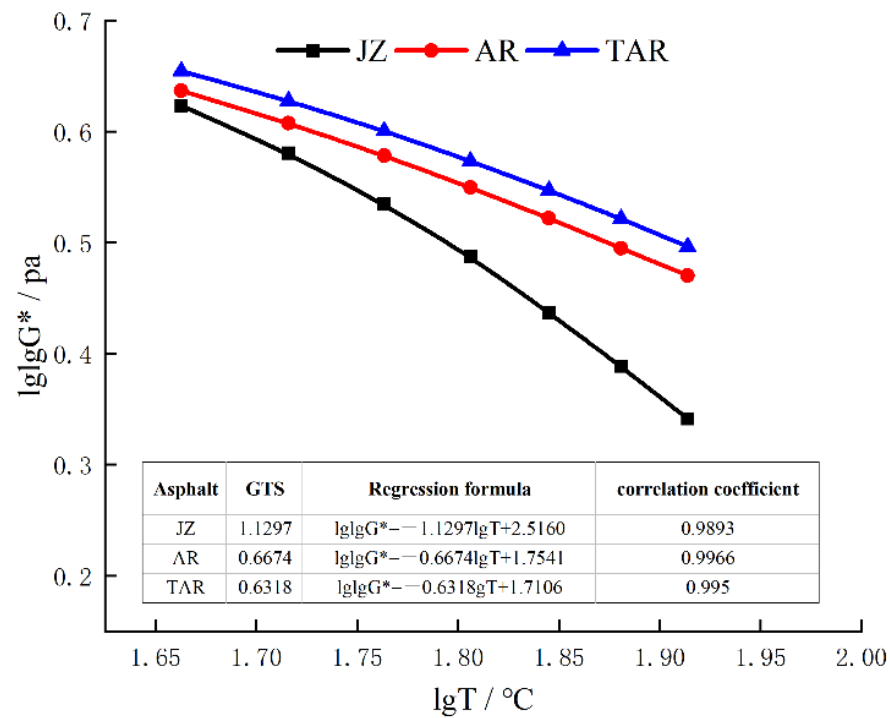


Figure 15. The variations of complex modulus G^* double logarithm with temperature logarithm.

3.2.3. Rutting Factor

In Figure 16, as the temperature increases, the rutting factors of the three kinds of asphalts exhibit decreasing trends. The reason is that asphalts behave as an elastic state at low temperature. As the temperature increases, the asphalt changes into a viscous flow state, and the strain caused by the shear force decreases gradually. Under the same temperature, the rutting factors are $TAR > AR > JZ$. When temperature is $64\text{ }^\circ\text{C}$, before the short-term aging, the rutting factors of AR and TAR increase by 2.3 and 0.6 times compared with JZ. The adding of crumb rubber enhances the rutting resistance of asphalts at high temperature. The reason is that the swelling effect of the compounds of asphalt and crumb rubber increases the elastic components of asphalt. Moreover, the addition of TOR enhances the interactions between asphalt and crumb rubber, so TOR enhances the deformation resistance of TAR at high temperature. At $58\text{ }^\circ\text{C}$, after the short-term aging, the rutting factors of the three kinds of asphalts increase by 0.8, 0.3, and 0.7 times, respectively. The reason is that the rutting factors increase after short-term aging, while AR is the least affected by short-term aging. Meanwhile, after short-term aging, the PG grading of AR is reduced by one grade. The final PG grading temperature of high temperatures are $64\text{ }^\circ\text{C}$ (JZ), $70\text{ }^\circ\text{C}$ (AR), and $82\text{ }^\circ\text{C}$ (TAR).

3.3. Low Temperature Performance Evaluation of Asphalt

3.3.1. Low Temperature Creep Test

According to the SHRP evaluation methods, the BBR test results of three kinds of asphalts are shown in Tables 11 and 12. When the temperature is $-12\text{ }^\circ\text{C}$, compared with m_{JZ} and S_{JZ} , m_{AR} increases by 19% and S_{AR} decreases by 73%. The results show that crumb rubber can enhance the relaxation ability at low temperature and crack resistance of asphalt. Under the same temperature, compared with AR and TAR, the m_{JZ} is slightly lower, and the S_{JZ} is slightly higher. In conclusion, the low temperature performances of the three kinds of asphalts are $AR > TAR > JZ$. According to the specification, the slope m of the creep curve is not less than 0.3, and the stiffness modulus S is not more than 300 MPa. The PG grading temperatures of low temperature can be obtained as $-22\text{ }^\circ\text{C}$ (JZ), $-34\text{ }^\circ\text{C}$ (AR), and $-28\text{ }^\circ\text{C}$ (TAR).

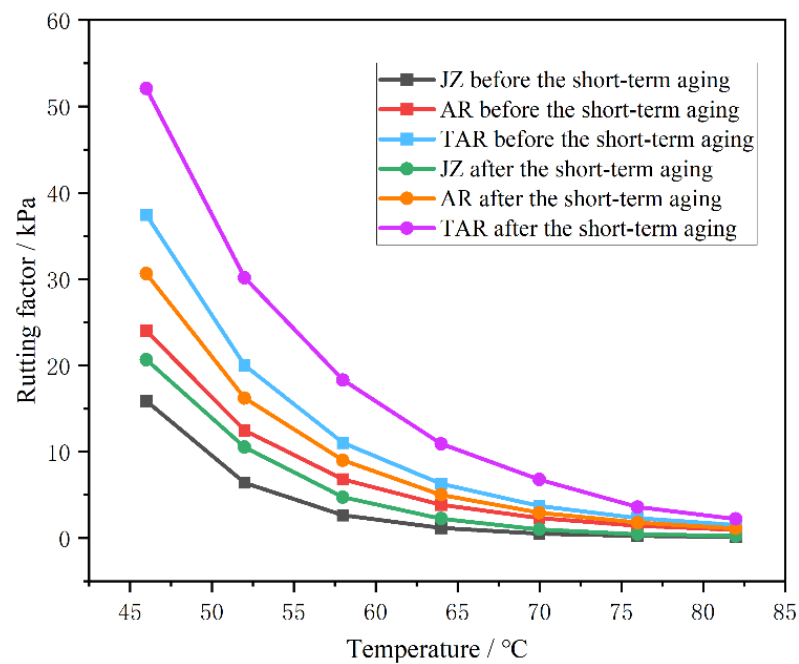


Figure 16. The effects of short-term aging on rutting factor.

Table 11. Low temperature bending test results of JZ.

Asphalt	−6 °C		−12 °C		−18 °C	
	m	S/MPa	m	S/MPa	m	S/MPa
JZ	0.449	47.6	0.365	123	0.286	296

Table 12. Low temperature bending test results of AR and TAR.

Asphalt	−12 °C		−18 °C		−24 °C		−30 °C	
	m	S/MPa	m	S/MPa	m	S/MPa	m	S/MPa
AR	0.436	33.7	0.378	80.6	0.358	235	0.232	455
TAR	0.42	43.1	0.343	106	0.297	253	0.236	430

Figure 17 shows the variations of creep rate and stiffness modulus changing with time. The creep rate decreases with the decrease in temperature, while the stiffness modulus increases. At the 87th load action, the creep rate curves of AR intersect at −18 and −24 °C, and then continue to accumulate with the number of load actions. However, $m_{-24^{\circ}\text{C}}$ is larger than $m_{-18^{\circ}\text{C}}$. It shows that PG grading cannot completely distinguish the low temperature performance of asphalt. It is limited to reflect the low temperature performance of asphalt only by m or S. Therefore, multiple processing and calculation methods should be used to evaluate [38–40].

3.3.2. m/S Value in Creep Compliance

The m/S ratio was adopted to evaluate the low temperature performance of asphalt. As the m/S ratio increases, the low temperature performance of asphalt is better [41,42].

Figure 18 shows the variations of m/S values with loading time. With the increase in loading time, the m/S values increase gradually and eventually tend to be flat. These show that the low temperature performances of three kinds of asphalts tend to be stable with the increase in loading time. At −12 °C, the m/S values of AR and TAR are significantly higher than JZ, indicating that the addition of crumb rubber improves the low temperature performance of asphalt. The m/S differences between AR and TAR decrease with decreas-

ing temperature. The results show that the effects of crumb rubber and TOR on the low temperature performance of asphalt are reduced at lower temperature.

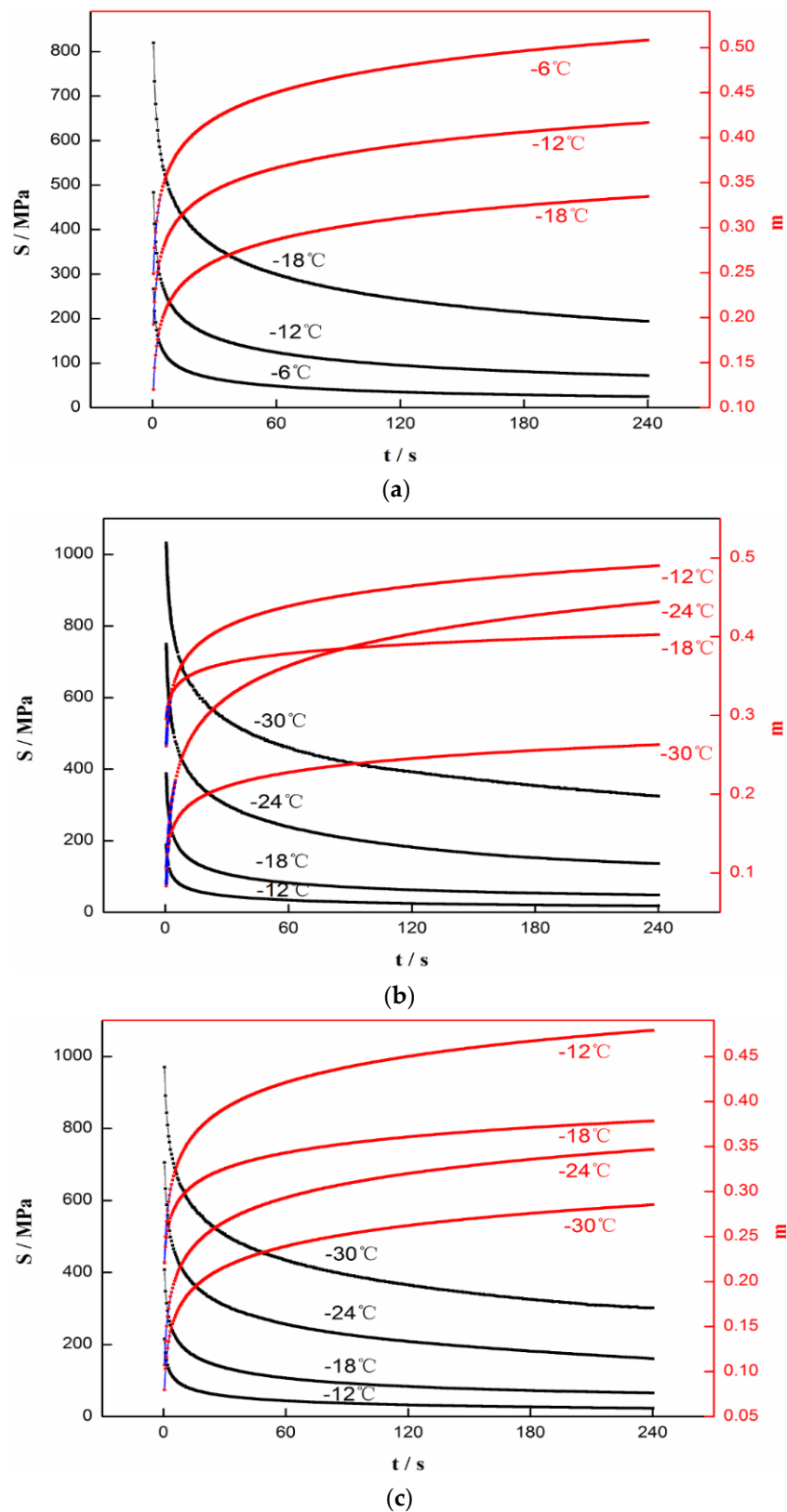


Figure 17. The variations of creep rate and stiffness modulus changing with time. (a) JZ, (b) AR, and (c) TAR.

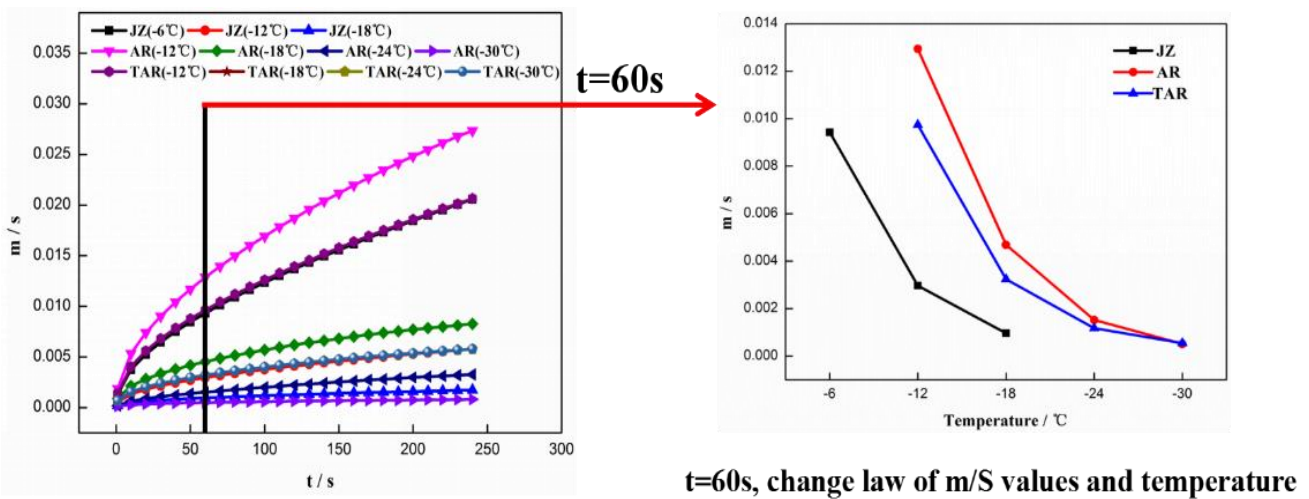


Figure 18. The variations of m/S values with loading time.

3.3.3. Determine Burgers Model Parameters

According to the creep compliance (Equation (6)) of Burgess model and the Levenberg–Marquardt (LM) method, the asphalt creep data were fitted. The elastic modulus (E_1, E_2) and viscosity coefficient (η_1, η_2) were obtained by fitting. The relaxation time (λ) and delay time (τ) were obtained according to Equations (7) and (8) [43–45]. Table 13 shows the Burgers model parameter results at different temperatures.

$$J(t) = \frac{1}{E_1} + \frac{1}{\eta_1}t + \frac{1}{E_2} \left(1 - e^{-\frac{E_2}{\eta_2}t} \right) \tag{6}$$

$$\lambda = \frac{\eta_1}{E_1} \tag{7}$$

$$\tau = \frac{\eta_2}{E_2} \tag{8}$$

in which $J(t)$ is creep compliance of Burgess model, Pa; E_1 is the elastic coefficient of Maxwell model, Pa; η_1 is the damping coefficient of Maxwell model, Pa; E_2 is the elastic coefficient of Kelvin model, Pa; η_2 is the damping coefficient of Kelvin model, Pa; and t is the load time, s.

Table 13. Burgers model parameter results at different temperatures.

Asphalt	Temperature (°C)	R ²	E ₁	E ₂	N ₁	N ₂	λ	τ
JZ	−6	0.9944	280.857	280.857	7461.986	1135.144	26.5686	4.0417
	−12	0.9928	285.224	2169.703	26,020.424	3365.985	91.2280	1.5514
	−18	0.9934	789.674	789.674	92,339.996	10,941.991	116.9343	13.8563
AR	−12	0.9934	199.717	199.717	5398.507	756.450	27.0308	3.7876
	−18	0.9915	385.665	385.665	17,037.055	2070.255	44.1758	5.3680
	−24	0.9952	723.123	723.123	48,590.296	7549.043	67.1951	10.4395
	−30	0.9369	956.527	956.527	191,557.173	19,670.318	200.2632	20.5643
TAR	−12	0.9939	222.573	222.573	7354.134	987.512	33.0414	4.4368
	−18	0.9913	388.469	388.469	25,389.389	3049.974	65.3576	7.8513
	−24	0.9945	667.333	667.333	72,246.635	8309.587	108.2617	12.4519
	−30	0.9940	905.090	905.090	159,510.036	17,540.130	176.2367	19.3794

Figures 19 and 20 show the relaxation time (λ) and delay time (τ) changes of the three kinds of asphalts at different temperatures. The relaxation time can represent the variation of stress in the material with time. The larger λ is, the lower the stress relaxation

ratio is, which is not conducive to rapid stress dissipation. Under the same temperature, the relaxation time of asphalts is $\lambda_{JZ} > \lambda_{TAR} > \lambda_{AR}$. The low temperature relaxation capacities of AR and TAR are much higher than JZ, because the blend of crumb rubber increases the viscosity of asphalt. TOR causes crumb rubber and asphalt to form network structures of large rings and chains polymers. At low temperatures, the intermolecular motion is difficult. The stress relaxation time is long.

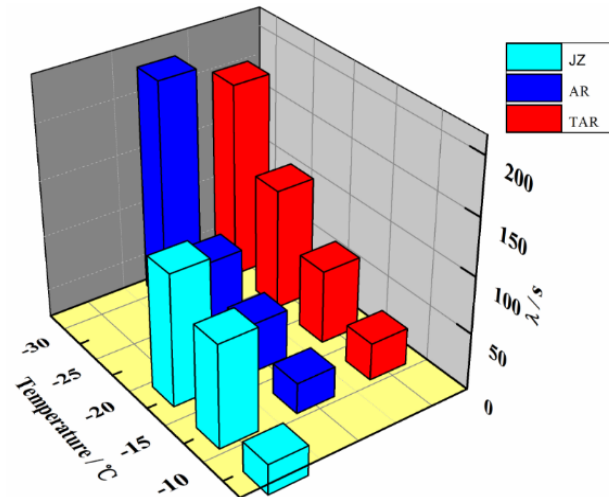


Figure 19. The variations of relaxation time (λ).

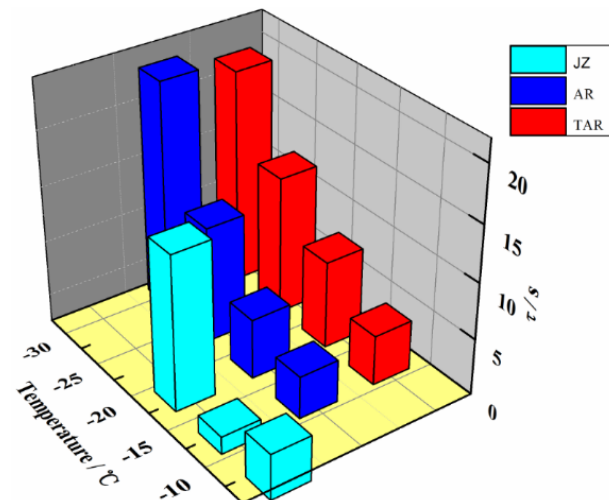


Figure 20. The variations of delay time (τ).

The relaxation time of asphalt increases with decreasing temperature. On one hand, with the decrease in temperature, the ratio of elastic component to viscous component in asphalt gradually increases. The energy consumption of asphalt under stress decreases. The relaxation capacity decreases, and the relaxation time increases. On the other hand, the molecular motion of the swelling crumb rubber polymer in asphalt is temperature dependent. At low temperatures, the internal friction of relative motion between molecular chains is larger, which leads to a longer stress relaxation time.

3.3.4. Dissipated Energy Ratio

Dissipated energy ratio is the ratio of dissipated energy to stored energy, which can reflect the stress relaxation capacity. The higher the ratio of dissipated energy, the better the stress relaxation capacity and low temperature performance will be. The dissipated energy ratio varies with time. According to the established storage energy (Equation (9))

and dissipated energy (Equation (10)), the dissipated energy ratio at $t = 60$ s was explored to analyze the low temperature performances of the three kinds of asphalts [46–48].

$$G_s(t) = \sigma_0^2 \left[\frac{1}{E_1} + \frac{1}{2E_2} \left(1 - 2e^{-\frac{E_2}{\eta_2}t} + e^{-\frac{2E_2}{\eta_2}t} \right) \right] \tag{9}$$

$$G_d(t) = \sigma_0^2 \left[\frac{1}{\eta_1}t + \frac{1}{2E_2} \left(1 - e^{-\frac{2E_2}{\eta_2}t} \right) \right] \tag{10}$$

in which $G_s(t)$ is storage energy; $G_d(t)$ is dissipated energy; E_1 is the elastic coefficient of Maxwell model, Pa; η_1 is the damping coefficient of Maxwell model, Pa; E_2 is the elastic coefficient of Kelvin model, Pa; η_2 is the damping coefficient of Kelvin model, Pa; t is the load time, s; and σ_0 is the stress, MPa.

Figure 21 is the variations of dissipated energy ratio at different temperatures. When the temperature decreases, the dissipated energy ratios of the three kinds of asphalts decrease gradually, and the reduction amplitudes also decrease gradually. These show that the elastic component of asphalt increases as the temperature decreases. When temperature is low, to a certain extent, the asphalt behaves as an elastomer. The stored energy increases in the asphalt, but the dissipated energy decreases. The stress relaxation capacity declines, which is not good for the crack resistance of AR and TAR at low temperature. Under the same temperature, the dissipated energy ratios of AR and TAR are much higher than JZ. The reason is that the adding of crumb rubber can enhance the energy dissipation in asphalt, and reduce the energy storage. Therefore, the stress relaxation capacity is enhanced. With the continuous decrease in temperature, the dissipated energy ratios of AR and TAR are close to the same, indicating that the influences of crumb rubber and TOR on the energy dissipation and storage capacity are much less than temperature.

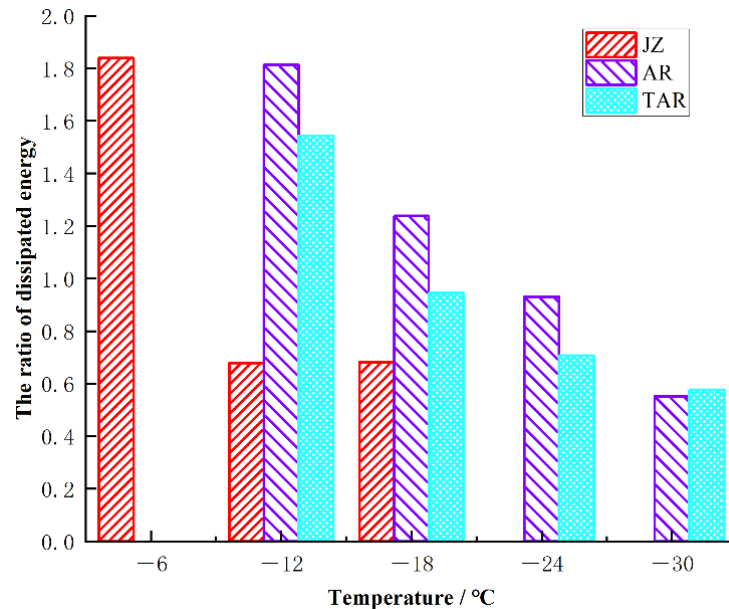


Figure 21. The variations of dissipated energy ratio at different temperatures.

3.3.5. Derivative of Creep Compliance

The derivative of creep compliance with respect to time reflects the change rate of creep compliance with time. The higher the derivative of creep compliance, the better the crack resistance of asphalt at low temperature. Equation (11) is the derivative of Equation (6), which is $J'(t)$ [48].

$$J'(t) = \frac{1}{\eta_1} + \frac{1}{\eta_2} e^{-\frac{E_2}{\eta_2}t} \tag{11}$$

According to Equation (11), $J'(t)$ values at different temperatures within 240 s were obtained. Its curves, changing with time, are shown in Figure 22.

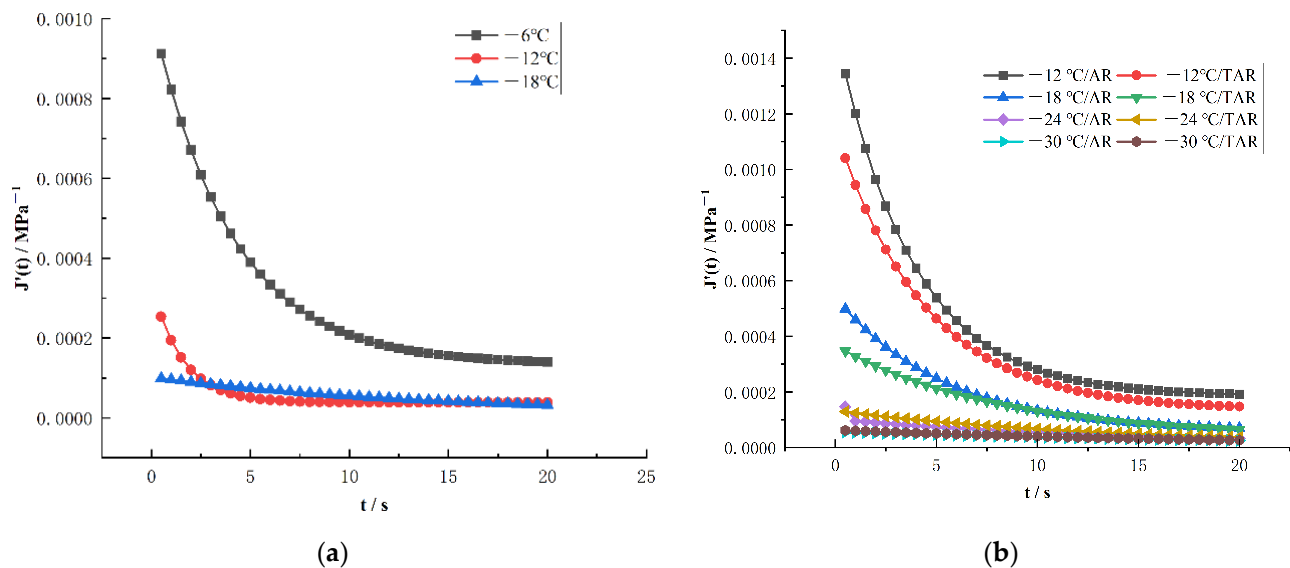


Figure 22. The variations of $J'(t)$ at different temperatures. (a) JZ (b) AR and TAR.

In Figure 22, with the increase in loading time, $J'(t)$ values gradually decrease and eventually tend to be stable. Therefore, the longtime load makes the low temperature crack resistances of asphalts tend to be stable, and the low temperature performances of three kinds of asphalts are no longer affected by the load action time. When the loading time is short, the $J'(t)$ values of the same asphalt decrease with the decrease in temperature. When the temperature is low, $J'(t)$ values tend to be stable, indicating that temperature has the most significant effect on the low temperature performances of three kinds of asphalts.

Based on viscoelastic theory and BBR creep test, the low temperature performances of JZ, AR, and TAR were evaluated and analyzed by m and S values, dissipated energy ratio, m/s value, and creep compliance derivative. The results of the four evaluation methods are consistent. The low temperature performances of the three kinds of asphalts are $AR > TAR > JZ$.

4. Microscopic Mechanism Analysis

Figure 23 shows fluorescence microscope images of three kinds of asphalts. The JZ is green-yellow. The additions of crumb rubber and TOR cause the color to deepen, so AR and TAR are dark green. The crumb rubber particles are black without fluorescence, and evenly disperse in the asphalt. TOR particles have no fluorescence effect and appear white. TOR particles evenly disperse in black crumb rubber particles–asphalt system. By comparing the colors of the fluorescent microscope images, it can be seen that the surface of crumb rubber particles absorbs the light components of asphalt, and the swelling effect is caused. The swelling effect promotes the degradation of crumb rubber. Degraded crumb rubber cross-links to form uniform network structures. Based on the characteristics of TOR, it can further enhance the swelling and network crosslinking effects of rubber-asphalt blend.

Figure 24 shows the scanning electron microscope images of AR and TAR. The crumb rubber particles are evenly dispersed in the asphalt system, but there is obvious difference in the interface between the asphalt and crumb rubber particles. In AR, the crumb rubbers are angular, and there are obvious gaps in the stacking place. In TAR, the swelling effects of asphalt and crumb rubbers are more sufficient. The interfaces of asphalt and crumb rubbers are seamless and integrated, indicating that TOR significantly enhances the compatibility of asphalt and crumb rubbers blending system.

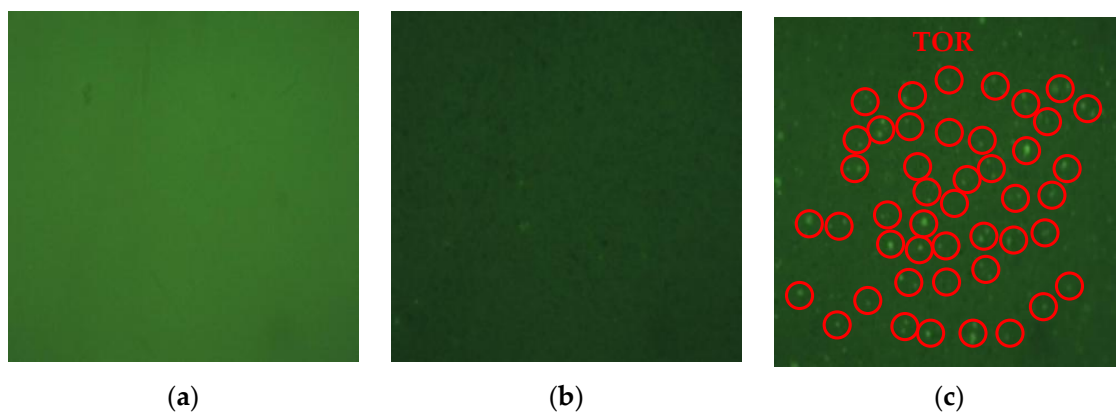


Figure 23. Fluorescent microscope images of asphalts. (a) JZ, (b) AR, and (c) TAR.

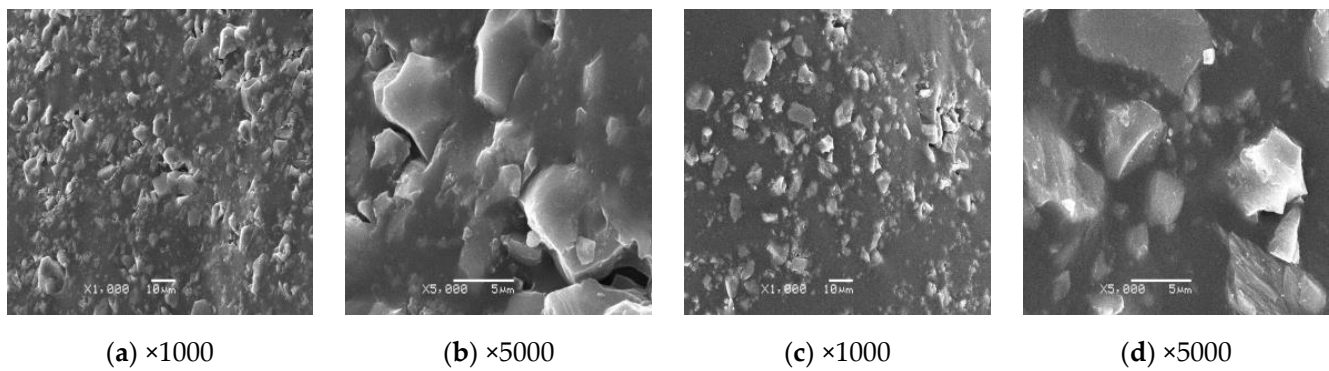


Figure 24. Scanning electron microscope images of the AR and TAR. ((a,b): AR. (c,d): TAR).

Figure 25 shows infrared spectrum diagrams of three kinds of asphalts. The infrared spectra diagrams of JZ, AR, and TAR are similar, indicating that the modification process is mainly physical modification. 1599 cm^{-1} is stretching vibration of C=C bond; 1456 cm^{-1} is the vibrational effect of the methylene $-\text{CH}_2-$ in-plane surface; and 1376 cm^{-1} is flexural vibration of C-H bond in $-\text{CH}_3-$. The benzene-ring substitution region of 1000 to 650 cm^{-1} is the vibrational effect of C-H and C-C bond of the benzene ring. Based on the infrared spectrum of crumb rubber and TOR, comparing the areas at the peak of curves, the absorption peak areas of AR and TAR at 1599 cm^{-1} decrease relatively, caused by the skeletal vibration of the conjugate double bond C=C of benzene ring. The main reason is the bending vibration of C-H bond of crumb rubber at 1400 cm^{-1} , indicating that there are weak chemical modification effects inside crumb rubber modified asphalt. The addition of TOR enhances the weak chemical interactions between crumb rubber and the asphalt interface to a certain extent.

Figure 26 shows the schematic diagram of AR and TAR asphalt molecular structure. Asphalt is composed of light components and asphaltene. When crumb rubber and asphalt are mixed at high temperatures, crumb rubber absorbs part of the light components in asphalt and expands in volume. The gel structure is formed around it. When TOR is added, the circular macromolecules and linear molecules of TOR intertwine with each other on the surface of crumb rubber, which gives TOR great deformation resistance and improved resilience after crosslinking.

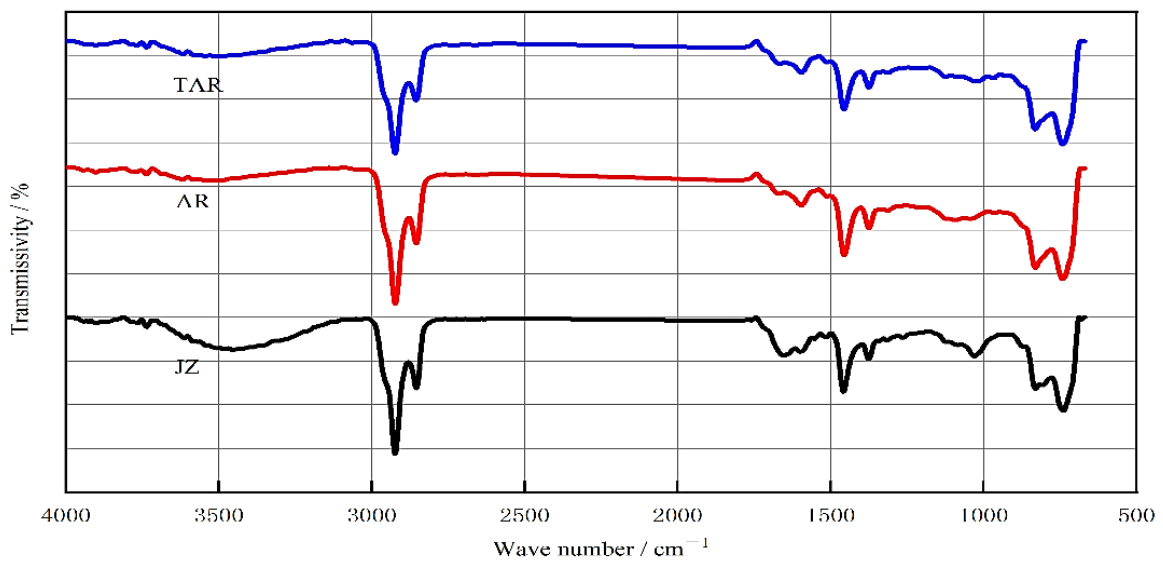


Figure 25. Infrared spectrum diagram of three kinds of asphalts.

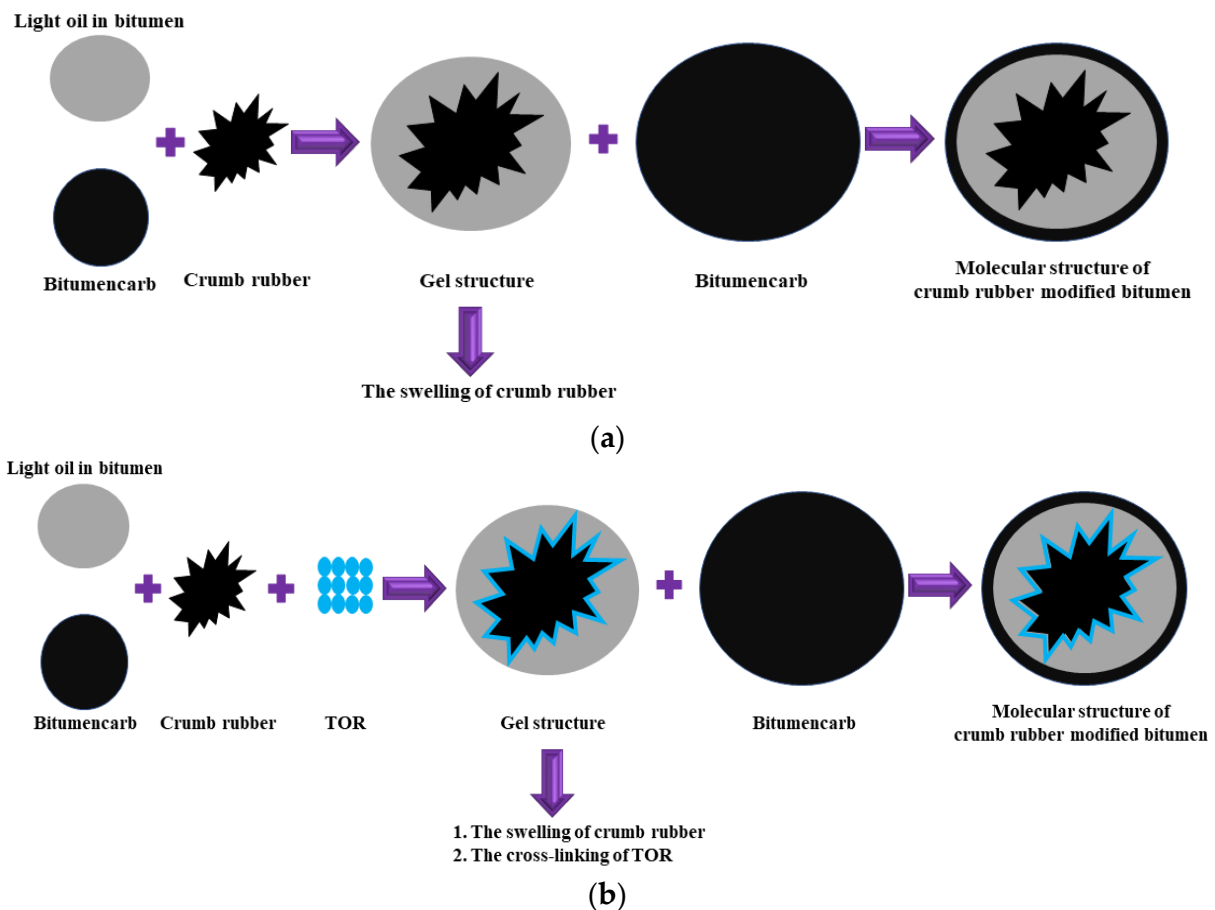


Figure 26. Schematic diagram of crumb rubber modified asphalt. (a) Schematic diagram of AR asphalt molecular structure. (b) Schematic diagram of TAR asphalt molecular structure.

5. Conclusions

In this study, the preparation process and parameters of crumb rubber modified asphalt suitable for alpine regions were proposed in detail. Meanwhile, the temperature susceptibility evaluations of matrix asphalt (JZ), crumb rubber modified asphalt (AR),

and crumb rubber modified asphalt blended with TOR (TAR) were investigated by multi-parameter. The following conclusions were drawn.

- The preparation process of crumb rubber modified asphalt (AR and TAR) suitable for alpine region was determined. Crumb rubber is selected 30 mesh, and the content is 24%. The preparation temperature and shearing rate are 205 °C and 5000 r/min, respectively. Shearing time is confirmed to be 60 min. TOR content is 4.5% of the quality of crumb rubber.
- PG grading is PG64-22 of JZ, PG70-34 of AR, and PG82-28 of TAR. The deformation resistance of TAR at high temperatures is superior to AR, but its crack resistance at low temperatures is relatively poor.
- The crumb rubber can improve the temperature susceptibility, and enhance its viscoelasticity at low temperatures. Meanwhile, the relaxation time is reduced. The dissipated energy and stress relaxation capacity are increased. Under the same temperature, the velocity of asphalt entering the creep stable phase decreases. The lower the temperature is, the less time it takes for asphalt to reach creep stability.
- When the crumb rubber is dispersed in the asphalt system, the surface of the crumb rubber absorbs the light components to produce swelling, and the network structures are cross-linked inside. If TOR is added, it can further enhance the swelling and network crosslinking effects of rubber–asphalt. In the asphalt system, the amount of precipitation of crumb rubber is reduced in a certain time. TOR, and the effects of desulfurization and depolymerization, enhance the storage stability in high temperature conditions.
- Based on the research results of temperature susceptibility of crumb rubber modified asphalt in alpine regions, its storage stability and weather resistance under the coupling effect of multiple factors should be further explored. The references for the design and construction of crumb rubber modified asphalt pavement are provided in alpine regions.

Author Contributions: Data curation, Y.T.; Formal analysis, M.C.; Investigation, Y.Z. (Youjie Zong); Methodology, R.X. and X.W.; Project administration, J.Y.; Software, Y.Z. (Yixing Zhang), B.F. and C.L.; Writing—original draft, H.W. All authors have read and agreed to the published version of the manuscript.

Funding: The authors wish to thank the financial support from the program of Scientific Innovation Practice Project of Postgraduates of Chang’an University in 2021, CHD. (No. 300103714063), and Provincial Undergraduate Innovation and Entrepreneurship Training Program in 2021, CHD. (No. S202110710332).

Institutional Review Board Statement: Not applicable.

Informed Consent Statement: Not applicable.

Data Availability Statement: The authors confirm that the data supporting the findings of this study are available within the article.

Conflicts of Interest: The authors declare no conflict of interest.

References

1. Wei, S.I.; Biao, M.A.; Nan, X.I.; Zeren, G.E. Compression characteristics of asphalt mixture under freeze-thaw cycles in cold plateau region. *J. Highw. Transp. Res. Dev.* **2013**, *30*, 6–10.
2. Gao, W.; Dong, N.; Wang, X.; Zeng, M. Test Analysis on Drainage Base Mixture of Asphalt Pavement in Cold Area. In *IOP Conference Series: Earth and Environmental Science*; IOP Publishing: Beijing, China, 2020; Volume 510, p. 052006.
3. Behnia, B.; Buttlar, W.G.; Reis, H. Cooling cycle effects on low temperature cracking characteristics of asphalt concrete mixture. *Mater. Struct.* **2014**, *47*, 1359–1371. [[CrossRef](#)]
4. Palit, S.K.; Reddy, K.S.; Pandey, B.B. Laboratory evaluation of crumb rubber modified asphalt mixes. *J. Mater. Civ. Eng.* **2004**, *16*, 45–53. [[CrossRef](#)]
5. Li, H.; Li, W.; Sheng, Y.; Lv, H. Influence of compound action of rubber powder and SBS on high-temperature performance of asphalt pavement surface. *J. Mater. Civ. Eng.* **2021**, *33*, 04021126. [[CrossRef](#)]

6. Ai, C.-F. Characteristics and Design Methods of Asphalt Pavement in Plateau-Cold Region. Diploma Thesis, Southwest Jiaotong University, Chengdu, China, 2008.
7. Liu, J.N.; Qi, L.; Wang, X.F.; Li, M.; Wang, Z.J. Influence of aging induced by mutation in temperature on property and microstructure development of asphalt binders. *Constr. Build. Mater.* **2022**, *319*, 126083. [[CrossRef](#)]
8. Liu, J.N.; Zhang, T.H.; Guo, H.Y.; Wang, Z.J.; Wang, X.F. Evaluation of self-healing properties of asphalt mixture containing steel slag under microwave heating: Mechanical, thermal transfer and voids microstructural characteristics. *J. Clean. Prod.* **2022**, *342*, 130932. [[CrossRef](#)]
9. Li, P.; Jiang, X.; Ding, Z.; Zhao, J.; Shen, M. Analysis of viscosity and composition properties for crumb rubber modified asphalt. *Constr. Build. Mater.* **2018**, *169*, 638–647. [[CrossRef](#)]
10. Wang, Q.Z.; Wang, N.N.; Tseng, M.L.; Huang, Y.M.; Li, N.L. Waste tire recycling assessment: Road application potential and carbon emissions reduction analysis of crumb rubber modified asphalt in China. *J. Clean. Prod.* **2020**, *249*, 119411. [[CrossRef](#)]
11. Erpeng, D.; Songlin, M.A.; Haimin, J. Asphalt pavement performance prediction model based on gray system theory. *J. Tongji Univ.* **2010**, *38*, 1161–1164.
12. Liu, W.; Xu, Y.; Wang, H.; Shu, B.; Barbieri, D.M.; Norambuena-Contreras, J. Enhanced Storage Stability and Rheological Properties of Asphalt Modified by Activated Waste Rubber Powder. *Materials* **2021**, *14*, 2693. [[CrossRef](#)]
13. Tao, M.A.; Chen, C.-L.; Zhang, Y.; Zhang, W.-G. Development of Using Crumb Rubber in Asphalt Modification: A Review. *China J. Highw. Transp.* **2021**, *34*, 1.
14. Picado-Santos, L.G.; Capitão, S.D.; Neves, J.M.C. Crumb rubber asphalt mixtures: A literature review. *Constr. Build. Mater.* **2020**, *247*, 118577. [[CrossRef](#)]
15. Ding, X.; Ma, T.; Zhang, W.; Zhang, D. Experimental study of stable crumb rubber asphalt and asphalt mixture. *Constr. Build. Mater.* **2017**, *157*, 975–981. [[CrossRef](#)]
16. Azizian, M.F.; Nelson, P.O.; Thayumanavan, P.; Williamson, K.J. Environmental impact of highway construction and repair materials on surface and ground waters: Case study: Crumb rubber asphalt concrete. *Waste Manag.* **2003**, *23*, 719–728. [[CrossRef](#)]
17. Shill, S.K.; Al-Deen, S.; Ashraf, M. Saponification and scaling in ordinary concrete exposed to hydrocarbon fluids and high temperature at military airbases. *Constr. Build. Mater.* **2019**, *215*, 765–776. [[CrossRef](#)]
18. Rocha Segundo, I.G.; Dias, E.A.; Fernandes, F.D.; Freitas, E.F.; Costa, M.F.; Carneiro, J.O. Photocatalytic asphalt pavement: The physicochemical and rheological impact of TiO₂ nano/microparticles and ZnO microparticles onto the bitumen. *Road Mater. Pavement Des.* **2019**, *20*, 1452–1467. [[CrossRef](#)]
19. Ding, X.; Chen, L.; Ma, T.; Ma, H.; Gu, L.; Chen, T.; Ma, Y. Laboratory investigation of the recycled asphalt concrete with stable crumb rubber asphalt binder. *Constr. Build. Mater.* **2019**, *203*, 552–557. [[CrossRef](#)]
20. Xiang, L.; Cheng, J.; Que, G. Microstructure and performance of crumb rubber modified asphalt. *Constr. Build. Mater.* **2009**, *23*, 3586–3590. [[CrossRef](#)]
21. Rocha Segundo, I.; Landi, S.; Margaritis, A.; Pipintakos, G.; Freitas, E.; Vuye, C.; Blom, J.; Tytgat, T.; Denys, S.; Carneiro, J. Physicochemical and rheological properties of a transparent asphalt binder modified with nano-TiO₂. *Nanomaterials* **2020**, *10*, 2152. [[CrossRef](#)]
22. Picado-Santos, L.G.; Capitão, S.D.; Dias, J.L.F. Crumb rubber asphalt mixtures by dry process: Assessment after eight years of use on a low/medium trafficked pavement. *Constr. Build. Mater.* **2019**, *215*, 9–21. [[CrossRef](#)]
23. Jamal, M.; Giustozzi, F. Low-content crumb rubber modified asphalt for improving Australian local roads condition. *J. Clean. Prod.* **2020**, *271*, 122484. [[CrossRef](#)]
24. Torretta, V.; Rada, E.C.; Ragazzi, M.; Trulli, E.; Istrate, I.A.; Cioca, L.I. Treatment and disposal of tyres: Two EU approaches. A review. *Waste Manag.* **2015**, *45*, 152–160. [[CrossRef](#)] [[PubMed](#)]
25. Li, J.; Zhu, Y.; Wang, H.; Wang, S.; Zhang, Y.; Zhang, Y. High temperature storage stability of asphalt modified with crumb rubber. *China Synth. Rubber Ind.* **2009**, *32*, 259–263.
26. Singh, D.; Sawant, D.; Xiao, F. High and Intermediate Temperature Performance Evaluation of Crumb Rubber Modified Binders with RAP. *Transp. Geotech.* **2016**, *10*, 13–21. [[CrossRef](#)]
27. Dias, J.L.F.; Picado-Santos, L.G.; Capitão, S.D. Mechanical performance of dry process fine crumb rubber asphalt mixtures placed on the Portuguese road network. *Constr. Build. Mater.* **2014**, *73*, 247–254. [[CrossRef](#)]
28. Yu, H.; Chen, Y.; Wu, Q.; Zhang, L.; Zhang, Z.; Zhang, J.; Miljković, M.; Oeser, M. Decision support for selecting optimal method of recycling waste tire rubber into wax-based warm mix asphalt based on fuzzy comprehensive evaluation. *J. Clean. Prod.* **2020**, *265*, 121781. [[CrossRef](#)]
29. Zhang, L.; Xing, C.; Gao, F.; Li, T.S.; Tan, Y.Q. Using DSR and MSCR tests to characterize high temperature performance of different rubber modified asphalt. *Constr. Build. Mater.* **2016**, *127*, 466–474. [[CrossRef](#)]
30. Chen, Z.; Wang, T.; Pei, J.; Amirhanian, S.; Xiao, F.; Ye, Q.; Fan, Z. Low temperature and fatigue characteristics of treated crumb rubber modified asphalt after a long-term aging procedure. *J. Clean. Prod.* **2019**, *234*, 1262–1274. [[CrossRef](#)]
31. Chen, S.; Gong, F.; Ge, D.; You, Z.; Sousa, J.B. Use of reacted and activated rubber in ultra-thin hot mixture asphalt overlay for wet-freeze climates. *J. Clean. Prod.* **2019**, *232*, 369–378. [[CrossRef](#)]
32. Fiore, N.; Caro, S.; D’Andrea, A.; Scarsella, M. Evaluation of asphalt modification with crumb rubber obtained through a high pressure water jet (HPWJ) process. *Constr. Build. Mater.* **2017**, *151*, 682–691. [[CrossRef](#)]

33. Ragab, M.; Abdelrahman, M. Enhancing the Crumb Rubber Modified Asphalt's Storage Stability through the Control of its Internal Network Structure. *Int. J. Pavement Res. Technol.* **2017**, *11*, 13–27. [[CrossRef](#)]
34. Chang, M.; Zhang, Y.; Pei, J.; Zhang, J.; Wang, M.; Ha, F. Low-Temperature Rheological Properties and Microscopic Characterization of Asphalt Rubbers Containing Heterogeneous Crumb Rubbers. *Materials* **2020**, *13*, 4120. [[CrossRef](#)] [[PubMed](#)]
35. Lu, Z.; Li, B.; Yang, X.; Wei, Y.; Zhang, Z. Production Process Parameter Optimization for Crumb Rubber Modified Asphalt Based on TOPSIS. *J. Highw. Transp. Res. Dev.* **2017**, *34*, 1–7.
36. Liang, M.; Xin, X.; Fan, W.; Sun, H.; Yao, Y.; Xing, B. Viscous properties, storage stability and their relationships with microstructure of tire scrap rubber modified asphalt. *Constr. Build. Mater.* **2015**, *74*, 124–131. [[CrossRef](#)]
37. Xiang, L.; Cheng, J.; Kang, S. Thermal oxidative aging mechanism of crumb rubber/SBS composite modified asphalt. *Constr. Build. Mater.* **2015**, *75*, 169–175. [[CrossRef](#)]
38. Wang, L.; Wang, Z.; Li, C. Low temperature performance of polyphosphoric acid asphalt based on viscoelastic theory. *Acta Mater. Compos. Sin.* **2017**, *34*, 322–328.
39. Hosseinneshad, S.; Kabir, S.F.; Oldham, D.; Mousavi, M.; Fini, E.H. Surface functionalization of rubber particles to reduce phase separation in rubberized asphalt for sustainable construction. *J. Clean. Prod.* **2019**, *225*, 82–89. [[CrossRef](#)]
40. Yang, X.; You, Z.; Hasan, M.R.; Diab, A.; Shao, H.; Chen, S.; Ge, D. Environmental and mechanical performance of crumb rubber modified warm mix asphalt using Evotherm. *J. Clean. Prod.* **2017**, *159*, 346–358. [[CrossRef](#)]
41. Liu, S.; Cao, W.; Shang, S.; Qi, H.; Fang, J. Analysis and application of relationships between low-temperature rheological performance parameters of asphalt binders. *Constr. Build. Mater.* **2010**, *24*, 471–478. [[CrossRef](#)]
42. Wang, S.; Guo, C.; Peng, F. Research on modified mechanism of asphalt with crumb tire rubber. *J. Chang. Univ.* **2010**, *4*, 34–38.
43. Wang, K.; Hao, P. Analysis of asphalt low temperature performance and viscoelasticity based on BBR test. *J. Liaoning Tech. Univ.* **2016**, *10*, 1138–1143.
44. Mashaan, N.S.; Ali, A.H.; Karim, M.R.; Abdelaziz, M. An overview of crumb rubber modified asphalt. *Int. J. Phys. Sci.* **2012**, *7*, 166–170.
45. Jeong, K.D.; Lee, S.J.; Amirghanian, S.N.; Kim, K.W. Interaction effects of crumb rubber modified asphalt binders. *Constr. Build. Mater.* **2010**, *24*, 824–831. [[CrossRef](#)]
46. Bocci, E.; Prospero, E. Recycling of reclaimed fibers from end-of-life tires in hot mix asphalt. *J. Traffic Transp. Eng.* **2020**, *7*, 678–687. [[CrossRef](#)]
47. Wang, H.; Ma, Z.; Chen, X.; Hasan, M.R.M. Preparation process of bio-oil and bio-asphalt, their performance, and the application of bio-asphalt: A comprehensive review. *J. Traffic Transp. Eng.* **2020**, *7*, 137–151. [[CrossRef](#)]
48. Liu, J.H. Experimental Study on Improving the Performance of Rubber with TOR. Diploma Thesis, Changsha University of Science and Technology, Changsha, China, 2019.